Biochem. J. (2012) **448**, 307–320 (Printed in Great Britain) doi:10.1042/BJ20121061

The activation loop of PKA catalytic isoforms is differentially phosphorylated by Pkh protein kinases in *Saccharomyces cerevisiae*

Steven HAESENDONCKX*†‡[1], Vanesa TUDISCA§[1], Karin VOORDECKERS†‡‖, Silvia MORENO§, Johan M. THEVELEIN†‡ and Paula PORTELA§[2]

*Department of Molecular Biology, University of Geneva CH-1211, Switzerland, †Laboratory of Molecular Cell Biology, Institute of Botany and Microbiology, KU Leuven, Kasteelpark Arenberg 31. B-3001 Leuven-Heverlee, Flanders, Belgium, ‡Department of Molecular Microbiology, VIB, Leuven-Heverlee, Flanders, Belgium, §Departamento de Química Biológica, Facultad de Ciencias Exactas y Naturales, Universidad de Buenos Aires, Ciudad Universitaria, Pabellón 2, Buenos Aires 1428, Argentina, and ‖VIB Laboratory for Systems Biology, Gaston Geenslaan 1, B-3001 Leuven, Belgium

PDK1 (phosphoinositide-dependent protein kinase 1) phosphorylates and activates PKA (cAMP-dependent protein kinase) *in vitro*. Docking of the HM (hydrophobic motif) in the C-terminal tail of the PKA catalytic subunits on to the PIF (PDK1-interacting fragment) pocket of PDK1 is a critical step in this activation process. However, PDK1 regulation of PKA *in vivo* remains controversial. *Saccharomyces cerevisiae* contains three PKA catalytic subunits, *TPK1*, *TPK2* and *TPK3*. We demonstrate that Pkh [PKB (protein kinase B)-activating kinase homologue] protein kinases phosphorylate the activation loop of each Tpk *in vivo* with various efficiencies. Pkh inactivation reduces the interaction of each catalytic subunit with the regulatory subunit Bcy1 without affecting the specific kinase activity of PKA. Comparative analysis of the *in vitro* interaction and phosphorylation of Tpks by Pkh1 shows that Tpk1 and Tpk2 interact with Pkh1 through an HM–PIF pocket interaction. Unlike Tpk1, mutagenesis of the activation loop site in Tpk2 does not abolish *in vitro* phosphorylation, suggesting that Tpk2 contains other, as yet uncharacterized, Pkh1 target sites. Tpk3 is poorly phosphorylated on its activation loop site, and this is due to the weak interaction of Tpk3 with Pkh1 because of the atypical HM found in Tpk3. In conclusion, the results of the present study show that Pkh protein kinases contribute to the divergent regulation of the Tpk catalytic subunits.

Key words: Bcy1, cAMP-dependent protein kinase (PKA), phosphoinositide-dependent protein kinase 1 (PDK1), PKB (protein kinase B)-activating kinase homologue (Pkh), *Saccharomyces cerevisiae*, Tpk.

INTRODUCTION

Protein kinases regulate the biological function and activity of other proteins via phosphorylation. In many cases, protein kinases are themselves regulated by phosphorylation. Within the family of protein kinases, a subfamily of AGC kinases, to which PKA (cAMP-dependent protein kinase), PKG (protein kinase G) and PKC (protein kinase C) belong, contains almost 15 % of all protein kinases encoded in the genome of both mammals and *Saccharomyces cerevisiae* [1].

Activation of these AGC kinases involves phosphorylation of two highly conserved regulatory motifs. The first motif, the PDK1 (phosphoinositide-dependent protein kinase 1) site, is located in the activation loop (also known as the T-loop) in the catalytic core, with the consensus sequence **T**FCGTXQY (the residue in bold indicates a phosphorylated residue, X is a variable residue) [2–4]. The second motif is located in the C-terminal tail extending from the catalytic domain and lies in the so-called HM (hydrophobic motif) with the consensus sequence FXXΦ**S/T**Φ (the residues in bold indicate phosphorylated residues, Φ indicates an aromatic residue) [4].

PDK1 belongs to this AGC family of protein kinases and is the activation loop kinase for several other members [5]. PDK1 can be recruited through the HM of its substrates via docking of this HM into a hydrophobic pocket, termed the PIF (PDK1-interacting fragment) [6,7]. Phosphorylation of the HM helps to position the HM within the PIF pocket, by binding to a nearby phosphate-binding pocket in PDK1 [3,7,8]. This docking mechanism has been proposed to enable PDK1 site phosphorylation of most substrates [7,9–11] (see Figure 8).

The catalytic subunits of mammalian PKA are phosphorylated on Thr[197] in the activation loop. This phosphorylation activates a nonphosphorylated recombinant catalytic subunit [12] and has been shown to be necessary for binding both the type I and II regulatory subunits [13]. However, whether PDK1 is the sole kinase responsible for this phosphorylation is controversial [14]. Evidence points to both autophosphorylation and PDK1-mediated phosphorylation of this residue as possible mechanisms [12,15].

The catalytic subunits of PKA contain a partial HM: they end in an FXXF motif. Despite this truncation, they can still interact with the PIF pocket of PDK1, and mutations in the HM diminish the interaction with and phosphorylation by PDK1 significantly *in vitro* [6,16]. Recently, the Thr[197] hydroxy group has been described as important for stabilizing the active site in the absence of phosphorylation [17].

Although several *in vitro* studies have investigated the mechanism of PKA phosphorylation by PDK1, little is known about the *in vivo* mechanism, particularly about effector-dependent changes in activation loop phosphorylation. Until now, the only stimulus known to regulate phosphorylation of PKA on Thr[197] is

Abbreviations used: DAPI, 4′,6-diamidino-2-phenylindole; GFP, green fluorescent protein; GST, glutathione transferase; HA, haemagglutinin; HM, hydrophobic motif; KD, kinase dead; PDK1, phosphoinositide-dependent protein kinase 1; PH, pleckstrin homology; PIF, PDK1-interacting fragment; PKA, cAMP-dependent protein kinase; PKH, PKB (protein kinase B)-activating kinase homologue; TM, turn motif; WT, wild-type.

[1] These authors contributed equally to this work.

[2] To whom correspondence should be addressed (email pportela@qb.fcen.uba.ar).

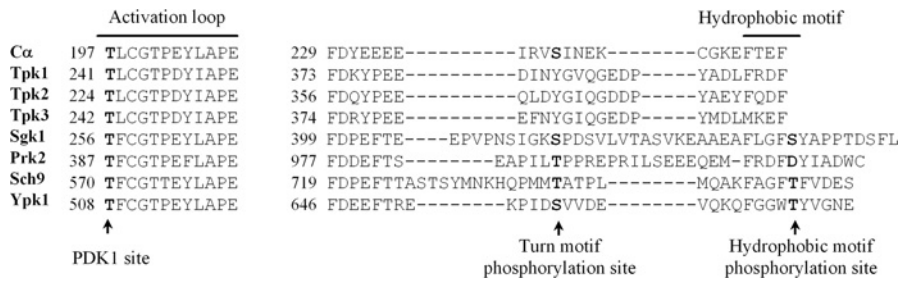

Figure 1 ***S. cerevisiae*** **PKA has motives that are conserved in PDK1 substrates**

Sequence alignment of selected PDK1 [Cα (ID 18747), Sgk1 (ID 6446) and Prk2 (ID 5585) from mammals] and Pkh [Sch9 (ID 856612) and Ypk1 (ID 853733)] substrates with the catalytic subunits of *S. cerevisiae* PKA [Tpk1 (ID 853275), Tpk2 (ID 855898) and Tpk3 (ID 853688)]. ID numbers are GenBank® accession numbers. Sequences corresponding to the PDK1 site in the activation loop (T-loop), the TM and the phosphorylation site in the C-terminal HM are shown, with phospho-acceptor residues in bold.

the engagement of TCR (T-cell receptor)/CD28 in T-cells. This mechanism seems to be only partially dependent on PDK1 [18].

In *S. cerevisiae*, PKA is a key player in several signal transduction pathways. As in other eukaryotes, *S. cerevisiae* PKA is a tetramer consisting of two regulatory subunits and two catalytic subunits. The regulatory subunit is encoded by *BCY1* and the catalytic subunits by *TPK1*, *TPK2* and *TPK3*. The conserved kinase domain of these three catalytic isoforms shares more than 75 % homology, whereas their N-terminal region is highly variable. Kinase activity of the catalytic subunits is inhibited by association with Bcy1, and this association is controlled by cellular cAMP levels. However, several studies have suggested the existence of cAMP-independent mechanisms that control PKA activity [19–23].

In *S. cerevisiae*, *PKH1/2/3* [PKH is PKB (protein kinase B)-activating kinase homologue] encode homologues of mammalian PDK1. Combined deletion of *PKH1/2* is lethal, due to a defect in cell wall integrity signalling. This lethality can be suppressed by expression of human PDK1 [4]. *PKH3*, which encodes the third PDK1 homologue, was originally isolated as a multicopy suppressor of the lethality of a temperature sensitive $pkh1^{ts}pkh2\Delta$ strain at the restrictive temperature [24]. A recent study shows that Pkh3 is required for sustaining PDK1 site phosphorylation in Sch9 [25]. The precise mechanism of regulation of Pkh protein kinases in yeast is still unclear. In contrast with PDK1, Pkh1/2 have no apparent PH (pleckstrin homology) domain known to bind PtdIns(3,4,5)P_3 or PtdIns(3,4)P_2 [26]. However, it appears that the Pkh protein kinases are capable of binding other phosphoinositides which are not recognized by a PH domain [4,27]. It has also been suggested that LCBs (long-chain bases), which are intermediates in *de novo* sphingolipid biosynthesis, could be potential regulators of Pkh protein kinases [28].

In addition to their role in cell wall integrity maintenance, Pkh1 and Pkh2 have been implicated in actin patch organization, endocytosis and eisosome assembly. These responses are mediated by Pkh targets, including Ypk1 and Ypk2, Pkc1 and Sch9 [29–36].

A recent report shows that Pkh1 phosphorylates the activation loop of Tpk1 (Thr^{241}) *in vitro* and that, *in vivo*, Pkh1–3 are required for Thr^{241} phosphorylation in newly synthesized Tpk1. Mutagenesis of Leu^{199} to glutamate in the PIF pocket of Pkh1, as well as mutations in one or both of the phenylalanine residues in the C-terminal FXXF motif to alanine in Tpk1, drastically reduces the Pkh1–Tpk1 interaction [25]. The same observation was made for the interaction between a mammalian catalytic subunit of PKA and PDK1 [6].

Mutation of Thr^{241} to alanine in the Tpk1 subunit reduces its affinity for the regulatory subunit approximately 30-fold and results in a monomeric cAMP-independent catalytic subunit [37]. Sequence alignment of several characterized Pkh substrates shows that Tpk2 and Tpk3 also contain a putative PDK1 site (Figure 1), where the possible target residues are Thr^{224} for Tpk2 and Thr^{242} for Tpk3. A phosphoproteomic study identified these residues as phosphorylated *in vivo* [38,39]. However, the upstream kinase, as well as the physiological role of this phosphorylation, remains elusive.

The present study identifies the Pkh protein kinases as the *in vivo* and *in vitro* PDK1 site kinases for each Tpk catalytic subunit, and analyses their contribution to cAMP-dependent catalytic activity. Our data suggest that each PKA catalytic subunit is differentially regulated by a common upstream Pkh kinase and that Pkh-mediated phosphorylation of Tpk is required for proper cAMP-dependent regulation of its kinase activity.

EXPERIMENTAL

Materials and reagents

Site-directed mutagenesis was performed using the QuikChange® site-directed mutagenesis kit (Stratagene). Blots were probed with anti-TPK1, anti-BCY1, anti-HA (haemagglutinin), anti-GFP (green fluorescent protein) (Santa Cruz Biotechnology) or anti-phospho-Thr^{241} phospho-specific polyclonal antibody (Eurogentec). Chemiluminescence Luminol reagent was from Santa Cruz Biotechnology.

Yeast strains, plasmids, medium and growth conditions

Yeast strains and plasmids used in the present study are described in Supplementary Tables S1 and S2 (at http://www.BiochemJ.org/bj/448/bj4480307add.htm) respectively. Site-directed mutagenesis was performed using the QuikChange® site-directed mutagenesis kit, and all constructs were sequenced. Yeast strains were transformed with the lithium acetate/PEG [poly(ethylene glycol)] method as described by Gietz et al. [40], with the exception that heat shock was done at 37 °C for temperature-sensitive strains. Transformants were selected on SD medium lacking the appropriate amino acid/nucleotide supplement for maintenance of the marker genes. Strains were grown on rich medium containing 2 % bactopeptone, 1 % yeast extract and 2 % glycerol (YPGly), 2 % galactose (YPGal) or 2 % glucose (YPGlu) at 24 °C. Synthetic media containing 0.67 % yeast nitrogen base without amino acids, 5 % ammonium sulfate, 2 % glucose (SD-Glu), 2 % glycerol (SD-Gly) or 2 % raffinose (SD-Raf) were used plus the necessary additions to fulfil auxotrophic requirements

and to maintain selectable plasmids. Solid medium contained 2 % agar. For Pkh inactivation, strains were grown at 24 °C to exponential phase (A_{600} of 0.3–0.6) and then shifted to 37 °C for 3 h. After heat-shock treatment, cell viability was verified by spot assay of serial dilutions on agar plates. Cell viability was determined as described previously [41]. Briefly, cells were incubated with Trypan Blue (10 mM) 5 min before microscopic observation. Dark blue cells were counted as dead cells. The precentage viability represents the proportion of viable cells. DAPI (4′,6-diamidino-2-phenylindole) staining was performed as described previously [42].

SDS/PAGE, slot blot and Western blot analysis

Samples of purified preparations or crude extracts were separated by SDS/PAGE (10 % T Laemmli system). Blots were probed with anti-TPK1, anti-BCY1, anti-HA and anti-GFP antibodies, or an anti-phospho-Thr^{241} phospho-specific polyclonal antibody (after validation it was referred to as anti-phospho-PDK1) which was generated against the synthetic phosphopeptide H_2N-VPDVTYT(PO_3H_2)LCGTPD-$CONH_2$. Specificity of the phospho-specific antibody against Thr^{224} in the PDK1 site of Tpk2 was assayed by slot blot. Synthetic phosphopeptides derived from phosphorylated Tpk1 [H_2N-VPDVTYT(PO_3H_2)LCGTPD-$CONH_2$] or Tpk2 [H_2N-VQTVTWT(PO_3H_2)LCGTPD-$CONH_2$] (generated by Eurogentec) or from their non-phosphorylated counterparts were spotted on to nitrocellulose membrane (Hybond, Amersham Bioscience). The blots were developed with Chemiluminescence Luminol reagent, and immunoreactive bands were visualized by autoradiography and analysed by digital imaging using a Bio-Imaging Analyser Bas-1800II. To quantify Western blots, short exposures of three independent experiments were scanned and quantified using Image Gauge 3.12 software.

Purification of HA-tagged proteins

WT (wild-type) + GFP–HA_3–Tpk1, *pkh1*^{ts}*pkh2*Δ*pkh3*Δ + GFP–HA_3–Tpk1 and WT + GFP–HA_3–$Tpk1^{T241A}$ strains were grown in SD-Glu medium at 24 °C and then shifted to 37 °C as indicated above. BJ2168 + Pkh1–HA and BJ2168 + $Pkh1^{KD}$–HA strains were grown in SD-Raf medium. Galactose at 2 % was added to the cultures and cells were harvested 4 h later. Cells were subsequently lysed by disruption with glass beads using the appropriate buffer [43]. Cell debris was pelleted by centrifugation at 15000 ***g*** for 5 min and the crude extract was used to immunoprecipitate HA-tagged proteins. The immunoprecipitation procedure was performed as described previously [43] using an anti-HA antibody. The immunoprecipitates were subjected to SDS/PAGE, transferred on to nitrocellulose and blotted with the appropriate antibodies: anti-phospho-PDK1, anti-Tpk1 or anti-HA. The co-immmunoprecipitated regulatory subunit was detected using anti-Bcy1.

Purification of His-tagged proteins

WT + GFP–Tpk1–His_6, WT + GFP–Tpk2–His_6, WT + GFP–Tpk3–His_6, *pkh1*^{ts}*pkh2*Δ*pkh3*Δ + GFP–Tpk1–His_6, *pkh1*^{ts}*pkh2*Δ*pkh3*Δ + GFP–Tpk2–His_6 and *pkh1*^{ts}*pkh2*Δ*pkh3*Δ + GFP–Tpk3–His_6 strains were grown in SD-Glu or SD-Gly medium at 24 °C and then shifted to 37 °C as indicated above. Cells were lysed by disruption with glass beads using the appropriate buffer [43]. Cell debris was pelleted by centrifugation at 15000 ***g*** for 5 min, and the crude extract was used to immunoprecipitate His-tagged proteins. The immunoprecipitation procedure was performed using Ni-NTA (Ni^{2+}-nitrilotriacetate) resin (Qiagen). The immunoprecipitates were subjected to SDS/PAGE, transferred on to nitrocellulose and blotted with anti-phospho-PDK1 and anti-GFP antibodies. The co-immunoprecipitated regulatory subunit was detected using an anti-Bcy1 antibody.

Purification of GST(glutathione transferase)-tagged proteins from *Escherichia coli*

The expression of GST-fused proteins was induced in the BL21 *E. coli* strain by addition of IPTG (isopropyl β-D-thiogalactopyranoside) to a final concentration of 0.3 mM. Cells were harvested after 3 h of growth at 30 °C and washed once with ice-cold PBS buffer. Cells were lysed by sonication in the appropriate buffer. Cell debris was pelleted by centrifugation at 15000 ***g*** for 10 min. The purification procedure was performed as described previously [25] using glutathione–Sepharose beads (GE Healthcare).

Pull-down assay

GST-fusion proteins were extracted as described above. The pull-down assay was performed as described previously [22]. Yeast extracts were incubated for 30 min with 50 μl of glutathione–Sepharose beads to reduce non-specific binding. Beads were collected and the resulting supernatant was incubated with an equal amount of bead-bound purified GST-fusion protein. The samples were solubilized by adding Laemmli sample buffer, subjected to SDS/PAGE and visualized by Coomassie Blue staining.

Kinase assay

Immunopurification of free and Bcy1-associated catalytic subunits of PKA was performed under standard assay conditions [43]. The kinase activity reaction was started by mixing the samples with assay mixture containing 0.15 mM ATP and 0.8 mM kemptide [43]. After 30 min at 30 °C, aliquots were processed according to the phosphocellulose paper method [44]. Protein kinase assays were linear with time and amount of kinase. Specific activity of PKA was calculated as the catalytic activity compared with the amount of immunoprecipitated TPK1-tagged protein quantified by densitometric analysis from equivalent samples subjected to SDS/PAGE followed by immunoblotting with anti-Tpk1 (Figure 2) or anti-GFP (Figure 4). The presence of an estimated maximum of 23 % untagged Tpk associated with Tpk-tagged species in a holoenzyme molecule did not affect PKA specific activity significantly since the specific activity of the purified samples from the WT strain in the presence of cAMP and *pkh*Δ strain were similar.

To verify that the PDK1 site was not being autophosphorylated as a consequence of the conditions used in the kinase assay, Tpk-purified proteins were subjected, after each assay, to SDS/PAGE and phosphorylation of the PDK1 site was analysed by Western blotting using phospho-specific antibodies.

Kinase assays using Pkh1–HA or $Pkh1^{KD}$–HA immunoprecipitated from crude extracts of the BJ2168 strain was performed as described previously [25]. Briefly, beads were resuspended in kinase buffer plus the appropriate immobilized purified GST substrate. Proteins were separated by SDS/PAGE. Gels were stained with Coomassie Blue and analysed by autoradiography using a PhosphoImager and by immunoblotting with anti-HA antibody.

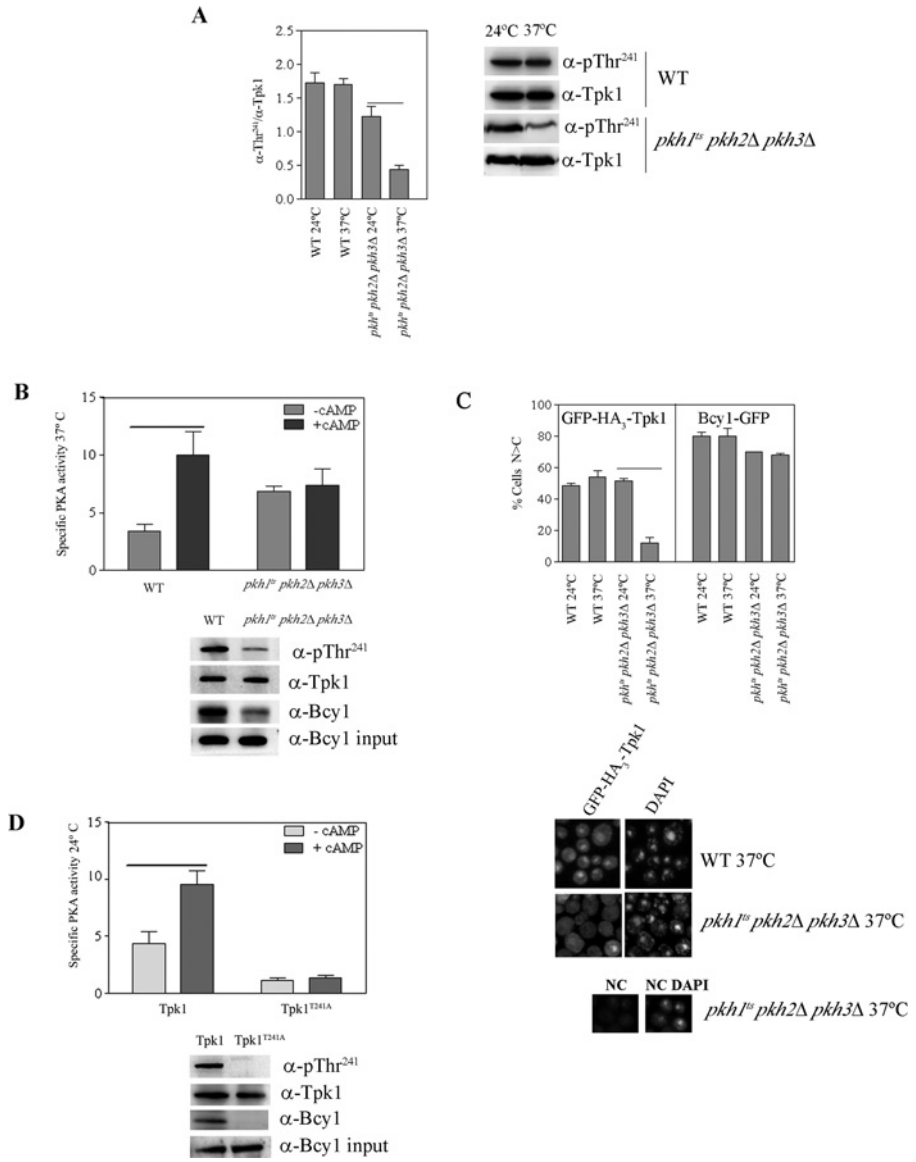

Figure 2 Pkh1 phosphorylates Tpk1 on its PDK1 site stimulating its interaction with Bcy1 *in vivo*

WT and *pkh1*^{ts}*pkh2*Δ*pkh3*Δ cells expressing GFP–HA_3–Tpk1 or GFP–Bcy1 were grown on SD-Gly at 24 °C and then shifted to 37 °C for 3 h or kept at 24 °C as a control. (**A**) The degree of phosphorylation of GFP–HA_3–Tpk1 was measured in immunoprecipitates by immunoblotting with an anti-phospho-Thr^{241} antibody and normalized to the total amount of Tpk1 detected using an anti-Tpk1 antibody. (**B**) Lower panel: the amount of Bcy1 associated with immunopurified GFP–HA_3–Tpk1 was determined by immunoblotting using an anti-Bcy1 antibody. Upper panel: PKA-specific activity assayed in immunoprecipitated GFP–HA_3–Tpk1 in the absence or presence of cAMP. Values were normalized to the total amount of Tpk1 detected by using an anti-Tpk1 antibody. (**C**) Localization of GFP–HA_3–Tpk1 or Bcy1–GFP was followed by fluorescence; in fixed aliquots of each culture; nuclei were stained with DAPI. NC represents autofluorescence of untransformed strains. Quantification of the number of 'N>C cells', with nuclear fluorescence stronger than cytoplasmic fluorescence, is shown in the left-hand panel. (**D**) Lower panel: the amount of Bcy1 associated with immunopurified GFP–HA_3–Tpk1 or GFP–HA_3–Tpk1^{T241A} was determined by immunoblotting using an anti-Bcy1 antibody. Upper panel: PKA specific activity of GFP–HA_3–Tpk1 and GFP–HA_3–Tpk1^{T241A} was assayed in the absence and presence of cAMP and normalized to total Tpk1 detected using an anti-Tpk1 antibody. The values for all of the experiments are the means ± S.D. from at least three independent assays. Horizontal lines denote significant differences ($P < 0.005$).

In situ PKA activity was measured using permeabilized cells in the presence of 10 μM cAMP as described previously [45].

Fluorescence microscopy

Cells used for fluorescence microscopy were grown to early exponential phase, fixed with 7.4 % formaldehyde, washed with PBS buffer and resuspended in 0.05 % Nonidet P40 plus 1 μg/ml DAPI for 30 min to stain the nuclei. Microscopy was performed using an epi-fluorescence microscope (Nikon Eclipse E600W). The images were processed using ImageJ (NIH) and Adobe Photoshop CS2 software. Quantification of fluorescence signals was performed by measuring pixel intensity in the nuclei and in an equivalent area of the cytoplasm and the background. Two categories of localization were distinguished: (i) N>C cells with nuclear fluorescence stronger than cytoplasmic fluorescence (nuclear to cytoplasm ratios of the signal >1.5) and (ii) N = C cells with fluorescence evenly distributed over the nucleus and cytoplasm (nuclear to cytoplasm ratios of the signal ⩽1.5).

Quantification of the protein half-life

Cultures (50 ml) of WT or *pkh1*^{ts}*pkh2*Δ*pkh3*Δ strains were grown in appropriate medium containing glucose or glycerol as the

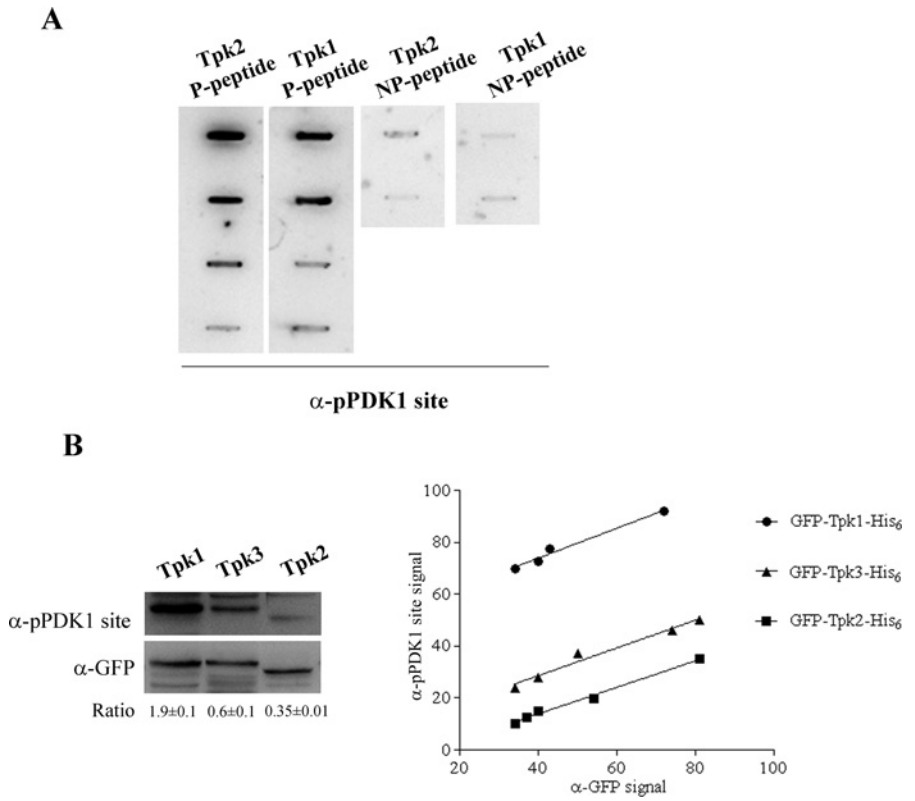

Figure 3 Tpk1, Tpk2 and Tpk3 show a differential degree of phosphorylation on their corresponding PDK1 sites *in vivo*

(**A**) Phosphorylated (P) synthetic peptides derived from Tpk1 and Tpk2 PDK1 sites were spotted as slot blots at decreasing concentration (4, 0.8, 0.08 and 0.016 nmol) and probed with an anti-phospho-Thr^{241} antibody. Non-phosphorylated (NP) Tpk1- and Tpk2-derived peptides were included as controls. (**B**) Increasing amounts of tag-purified GFP–Tpk1–His$_6$, GFP–Tpk2–His$_6$ and GFP–Tpk3–His$_6$ were analysed by Western blot using anti-phospho-PDK1 and anti-GFP antibodies. The correlation of the intensity of the anti-phospho-PDK1 compared with anti-GFP determined by densitometric analysis (in arbitrary units) was represented in a graph and the slopes calculated. GFP–Tpk1–His$_6$ slope: 0.32, $r^2 = 0.98$; GFP–Tpk2–His$_6$ slope: 0.43, $r^2 = 0.99$; and GFP–Tpk3–His$_6$ slope: 0.37, $r^2 = 0.96$. Representative Western blots are shown. Values represent the ratio of anti-phospho-PDK1/anti-GFP signal. Values are means ± S.D. ($n = 4$; $P < 0.05$)

carbon source to exponential phase. The cultures were shifted to 37 °C for 30 min or maintained at 24 °C before the addition of cycloheximide. Cycloheximide, a translation inhibitor, was added to a final concentration of 35 μg/ml to inhibit protein synthesis. After cycloheximide treatment, an equal amount of cells was collected at 0, 30, 60, 90 and 120 min, and cell lysates were prepared as described previously [46]. Two aliquots of extracts were analysed by SDS/PAGE and Western blotting as described above. The band corresponding to Tpk1 was detected using anti-Tpk1 or anti-GFP antibodies. At least two exposure times (1 min and 5 min) with the Bio-Imaging Analyzer Bas-1800II were analysed. After cycloheximide treatment, cell viability was verified by a spot assay of serial dilutions on agar plates.

Reproducibility of the results

All of the experiments were repeated several times (indicated in each Figure) with independent cultures and enzyme preparations. The *in vitro* PKA activity (Figures 2B, 2D and 4B) was analysed using *t*-test-dependent samples. The subcellular localization (Figure 2C) and densitometric analysis of proteins (Figure 2A) was analysed using *t*-test-independent samples. Densitometric analysis of the phosphorylation degree of Tpk proteins (Figures 3C and 4A) and the amount of co-immunoprecipitated Bcy1 (Figure 4A) was analysed using the ANOVA-Tukey HSD (honestly signifcant difference) test (α 0.05). Statistical analysis of the results in Figure 4(A) are: Tpk1 WT at 24 °C compared with Tpk2 WT at 24 °C compared with Tpk3 WT at 24 °C, $^{*}P < 0.05$; Tpk1 WT at 24 °C compared with Tpk1 WT at 37 °C, Tpk2 WT at 24 °C compared with Tpk2 WT at 37 °C, Tpk3 WT at 24 °C compared with Tpk3 WT at 37 °C, $P > 0.05$; Tpk2 WT at 24 °C compared with Tpk2 *pkh1^{ts}pkh2*Δ*pkh3*Δ at 24 °C, Tpk2 *pkh1^{ts}pkh2*Δ*pkh3*Δ at 24 °C compared with Tpk2 *pkh1^{ts}pkh2*Δ*pkh3*Δ at 37 °C, $^{*}P < 0.05$; Tpk3 WT at 24 °C compared with Tpk3 *pkh1^{ts}pkh2*Δ*pkh3*Δ at 24 °C, Tpk3 *pkh1^{ts}pkh2*Δ*pkh3*Δ at 24 °C compared with Tpk3 *pkh1^{ts}pkh2*Δ*pkh3*Δ at 37 °C, $^{*}P <$ 0.05. Statistical analysis of the results in Figure 4(B) are: Tpk1 WT at 24 °C compared with Tpk3 WT at 24 °C, $^{***}P < 0.05$; Tpk2 WT at 24 °C compared with Tpk3 WT at 24 °C, $^{***}P <$ 0.05; Tpk2 WT at 24 °C compared with Tpk2 *pkh1^{ts}pkh2*Δ*pkh3*Δ at 24 °C, $^{***}P < 0.05$; Tpk2 *pkh1^{ts}pkh2*Δ*pkh3*Δ at 24 °C compared with Tpk2 *pkh1^{ts}pkh2*Δ*pkh3*Δ at 37 °C, $^{*}P < 0.05$; and Tpk1 *pkh1^{ts}pkh2*Δ*pkh3*Δ at 24 °C compared with Tpk1 *pkh1^{ts}pkh2*Δ *pkh3*Δ at 37 °C, $^{*}P < 0.05$.

RESULTS

Inactivation of Pkh protein kinases reduces phosphorylation of Thr^{241} in Tpk1 and impairs its inactivation by Bcy1

It has been shown previously that Thr^{241}, located in the activation loop of Tpk1, is phosphorylated *in vitro* by Pkh1 [25]. *In vivo* this phosphorylation occurs during or shortly after synthesis of Tpk1. Once this phosphorylation has occurred, it is very stable and is not

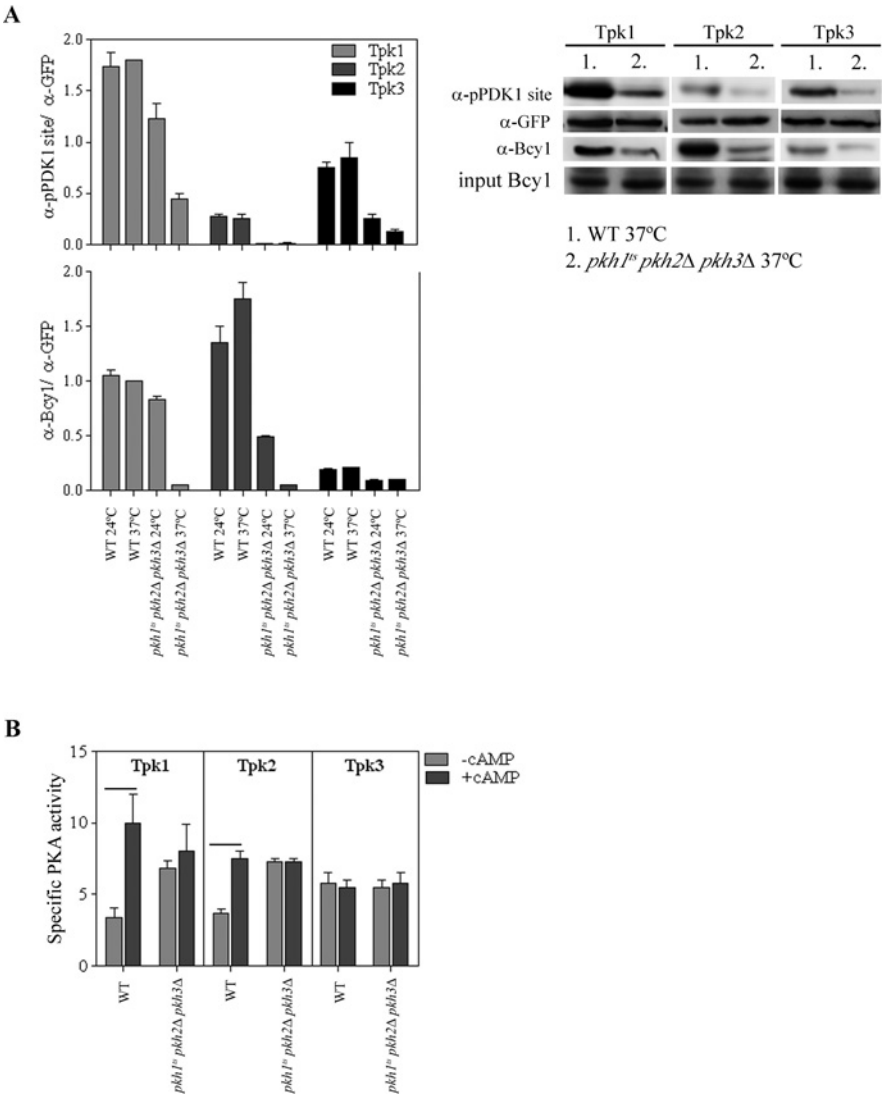

Figure 4 Pkh1 phosphorylates Tpk2 and Tpk3 on their PDK1 site *in vivo*

(**A**) Cells of the WT and *pkh1*^{ts}*pkh2*Δ*pkh3*Δ strain expressing GFP–Tpk1–His_6, GFP–Tpk2–His_6 or GFP–Tpk3–His_6 were grown on SD-Glu at 24 °C and then shifted to 37 °C or kept at 24 °C as a control for 3 h. The tagged proteins were immunopurified from cell extracts and PDK1 site phosphorylation was analysed by immunoblotting with an anti-phospho-PDK1 antibody. The regulatory subunit associated with each purified GFP–Tpk–His_6 was detected by immunoblotting using an anti-Bcy1 antibody. The total amount of catalytic subunit loaded was determined by immunoblotting using an anti-GFP antibody (right-hand panel). The histograms show the ratio of anti-phospho-PDK1/anti-GFP (upper panel) and anti-Bcy1/anti-GFP (lower panel) derived from densitometric analysis of the bands. Values are the means ± S.D. from two independent immunoprecipitation assays. Statistical analysis has been detailed in the Experimental section. (**B**) Protein kinase activity (± cAMP) was assayed in equivalent aliquots of the immunopurified Tpk1, Tpk2 and Tpk3 samples isolated from cells of the WT and *pkh1*^{ts}*pkh2*Δ*pkh3*Δ strain shifted for 3 h to 37 °C. Specific activity was estimated as described for Figure 2. Values are the means ± S.D. from two independent immunoprecipitation assays. Horizontal lines over specific activity with and without cAMP of immunoprecipitated samples denote significant differences ($P < 0.005$).

affected by the addition of glucose or nitrogen to cells deprived of these nutrients, nor is it abolished by *in vitro* alkaline phosphatase treatment [20]. To study the effect of abolishing phosphorylation on this site, we used a tagged version of Tpk1 (GFP–HA_3–TPK1) expressed in a WT strain and in a thermosensitive strain, *pkh1*^{ts}*pkh2*Δ *pkh3*Δ, in which Pkh activity could be inactivated at restrictive temperature. The incubation time at the restrictive temperature was chosen based on the reported stability of Thr^{241} phosphorylation together with our own data on the half-life of both tagged and untagged Tpk1 of ≈120 min (results not shown). An incubation time of 3 h at 37 °C was selected, after verifying that this time did not affect the overall cellular fitness of both strains [as judged by cell viability (Supplementary Figure S1A), Trypan Blue accumulation (Supplementary Figure S1C) and the absence of apoptotic nuclei (Supplementary Figure S1D) (at http://www.BiochemJ.org/bj/448/bj4480307add.htm)] and that the expression of both tagged and untagged Tpk1, as well as of Bcy1, did not change at the restrictive temperature (Supplementary Figure S2A at http://www.BiochemJ.org/bj/448/bj4480307add.htm). We have previously verified that epitope tagging of PKA subunits does not affect their catalytic activity [47].

In vivo phosphorylation of Thr^{241} was monitored by immunopurification of the protein with anti-HA antibody and immunoblotting using a phospho-specific antibody (α-phospho-Thr^{241}) in WT and mutant strains before and after 3 h incubation at the restrictive temperature. Figure 2(A) shows that phosphorylation of Thr^{241} is significantly reduced

(approximately 70 %) in a *pkh1*^{ts} *pkh2*Δ *pkh3*Δ strain at restrictive temperature. We further analysed the importance of *in vivo* Thr^{241} phosphorylation for Tpk1 catalytic activity and its interaction with the regulatory subunit Bcy1. This was done by measurement of catalytic activity (±cAMP) (Figure 2B, top panel) and by detection of Bcy1 in the anti-HA immunoprecipitate (Figure 2B, bottom panel). As judged from the specific activity of PKA, measured in the presence of cAMP, the catalytic activity of Tpk1 was not significantly different ($P > 0.05$) when phosphorylation of Thr^{241} was strongly reduced, indicating that Pkh inactivation had no impact on the turnover number of the enzyme. Care was taken to use saturating concentrations of both the peptide substrate kemptide and ATP (0.8 and 0.15 mM respectively) in the activity assay, according to the kinetic parameters reported for Tpk1^{T241A} [48]. As shown in Figure 2(B) (bottom panel), a decrease in Tpk1 Thr^{241} phosphorylation reduced the Tpk1–Bcy1 interaction. In agreement with this observation, the Tpk1 kinase activity in the immunoprecipitate from WT cells was dependent on cAMP addition (±cAMP kinase activity, 0.3), than in the absence of Pkh activity, where the enzyme is no longer inhibited by its regulatory subunit and already active (±cAMP kinase activity, 1).

To further investigate whether Pkh inactivation has an impact on other properties of Tpk1, GFP–HA$_3$–Tpk1 localization was analysed. In exponentially growing cells, Tpk1 has a nucleo-cytoplasmic distribution [47,49], with a nuclear localization dependent on its interaction with a properly localized Bcy1 [50]. Figure 2(C) shows that subcellular localization of GFP–HA$_3$–Tpk1 in WT cells, rapidly growing on glucose, is both nuclear and cytoplasmic (50 % cells N>C) at 24 °C and 37 °C. In the *pkh1*^{ts} *pkh2*Δ *pkh3*Δ strain, incubated at 24 °C, Tpk1 has a similar nucleo-cytoplasmic distribution. However, after inactivation of Pkh1 in the *pkh1*^{ts} *pkh2*Δ *pkh3*Δ strain by incubation at the restrictive temperature, GFP–HA$_3$–Tpk1 was relocalized to the cytoplasm. In contrast, Bcy1–GFP localization was mainly nuclear in all strains and conditions analysed. These results suggest that the absence of nuclear accumulation of Tpk1 upon Pkh inactivation, when Tpk1 is not phosphorylated on its PDK1 site, could be due to its reduced interaction with Bcy1.

Taken together, the results shown in Figures 2(A)–2(C) suggest that, *in vivo,* Pkh protein kinases regulate cAMP-dependent Tpk1 activity by controlling its association with Bcy1, rather than by affecting its catalytic turnover number.

The *in vivo* importance of the threonine residue itself at position 241 was evaluated using the mutant Tpk1^{T241A}. Previous *in vitro* data indicate that mutation of Thr^{241} to Ala^{241} in Tpk1 has two opposite effects on kinase activity: it decreases interaction with Bcy1 while severely reducing kinase activity [25,37]. Protein abundance and half-life of Tpk1 do not seem to depend on Thr^{241} since the Tpk1^{T241A} mutant displays a half-life similar to WT Tpk1 and is present at similar levels (results not shown). We assayed the specific kinase activity of immunopurified GFP–HA$_3$–Tpk1 and GFP–HA$_3$–Tpk1^{T241A}, following the same strategy used for Figure 2(B) (Figure 2D). Comparison of the results from Figures 2(B) and 2(D) clearly shows that GFP–HA$_3$–Tpk1^{T241A} has a much lower catalytic activity (measured in the presence of cAMP) not only when compared with a phosphorylated GFP–HA$_3$–Tpk1 isolated from either a WT strain (at 24 °C and 37 °C) or from *pkh1*^{ts} *pkh2*Δ *pkh3*Δ at the permissive temperature, but also when compared with a much less phosphorylated GFP–HA$_3$–Tpk1 obtained from cells in which Pkh had been inactivated at 37 °C (Figure 2B). As expected, the kinase activity assayed in the absence and presence of cAMP (±cAMP activity, 1 in mutant and 0.4 in WT), shows that the subunit does not respond to cAMP due to the known decrease in interaction of the GFP–HA$_3$–Tpk1^{T241A} mutant with Bcy1 [48].

The difference in catalytic activity of an under-phosphorylated Tpk1 when compared with a T241A mutation is also known to occur in mammalian Cα [17]. This suggests an important role of the hydroxy group of Thr^{241} in Tpk1 for the conformation of the active enzyme, as has been shown to occur in Cα [17].

Therefore the experimental approach of reducing Thr^{241} phosphorylation in Tpk1 *in vivo* by inactivation of the Pkh protein kinases in order to study the *in vivo* implications of the phosphorylation state of Tpk1 seems to be more suitable than the mutation of Thr^{241} to alanine.

PKA catalytic subunits show a different degree of phosphorylation at their activation loop

In order to make a comparative analysis and to determine whether Tpk1, Tpk2 and Tpk3 are all phosphorylated on the corresponding threonine residue in the activation loop, GFP–Tpk1–His$_6$, GFP–Tpk2–His$_6$ and GFP–Tpk3–His$_6$, purified from exponentially growing cells on glucose, were subjected to Western blot analysis using the anti-phospho-Thr^{241} antibody (also referred to as the anti-phospho-PDK1 site antibody) (Figure 3). The sequence surrounding the phosphorylatable threonine residue in the activation loop is identical for Tpk1 and Tpk3 and slightly different for Tpk2 (Figure 1). Slot blot assays confirm that the antibody has the same specificity for both phosphorylated Thr^{241} in Tpk1 and Thr^{224} in Tpk2 (Figure 3A). We verified that anti-phospho-PDK1 had a similar relative affinity for each phospho-GFP–Tpk–His$_6$ full-length protein, since the slopes of anti-phospho-PDK1 compared with anti-GFP densitometric signals of purified proteins in Western blots were almost identical (Figure 3B, right-hand panel). However, the degree of phosphorylation of Thr^{242}-Tpk3 and particularly Thr^{224}-Tpk2 is much lower than that of Thr^{241}-Tpk1 (Figure 3B, left-hand panel, α-pPDK1/α-GFP ratio). A similar result was obtained using proteins purified from glycerol-grown cells (results not shown), suggesting that the phosphorylation of this residue is not regulated by the carbon source, at least under these conditions.

From these results it can be concluded that each Tpk catalytic subunit undergoes a different degree of phosphorylation on the PDK1 site *in vivo*, with Tpk1>Tpk3>Tpk2.

Inactivation of Pkh activity reduces PDK1 site phosphorylation in all three Tpks *in vivo*

As shown above, *in vivo* phosphorylation by the Pkh protein kinases is required for the Tpk1–Bcy1 interaction. To determine whether the Pkh protein kinases have a similar regulatory role for Tpk2 and Tpk3, we used the same strategy as for Tpk1 (Figure 4). Since Tpk2 and Tpk3 have a half-life of ≈80 min both at 24 °C and 37 °C (results not shown), the same incubation time at 37 °C (Pkh inactivation) as for Tpk1 was considered suitable. For comparative analysis, GFP–Tpk1–His$_6$, GFP–Tpk2–His$_6$ and GFP–Tpk3–His$_6$ were purified from glucose-grown WT and *pkh1*^{ts} *pkh2*Δ *pkh3*Δ cells at 24 °C or after 3 h incubation at 37 °C. Cell viability after heat shock was similar for all strains, as tested by spot assay (Supplementary Figure S1B). No major differences were found in the relative protein level for Bcy1 in the *pkh1*^{ts} *pkh2*Δ *pkh3*Δ and WT strains expressing GFP–Tpk–His$_6$ compared with untransformed strains (Figure 4 and Supplementary Figure S2A).

In vivo phosphorylation of the threonine residue in the activation loop of Tpk1, Tpk2 and Tpk3 was quantified by densitometric analysis of the anti-phospho-PDK1 site and

anti-GFP signals (Figure 4A, right-hand panel). The low phosphorylation level of the PDK1 site in Tpk2 and Tpk3 observed in the WT strain was almost completely abolished under both permissive and restrictive conditions in cells of the *pkh1^{ts} pkh2*Δ *pkh3*Δ mutant (Figure 4A, left-hand panel). These results indicate that the Pkh protein kinases are required for PDK1 site phosphorylation of all three PKA catalytic subunits *in vivo*. Differential reduction in PDK1 phosphorylation of the Tpk isoforms in WT compared with *pkh1^{ts} pkh2*Δ *pkh3*Δ cells could easily be detected at permissive temperature: 30 % for Tpk1, 90 % for Tpk2 and 70 % for Tpk3. At restrictive temperature, PDK1 site phosphorylation of both Tpk2 and Tpk3 was completely abolished. Taken together, these results suggest that each Tpk can be phosphorylated with different catalytic efficiencies by the Pkh protein kinases *in vivo*.

As shown in Figure 2, reduction in Pkh-mediated phosphorylation in Tpk1 is accompanied by a reduced interaction with Bcy1 *in vivo*. We examined association of Tpk2 and Tpk3 with Bcy1 by co-immunoprecipitation from cells of the WT or *pkh1^{ts} pkh2*Δ *pkh3*Δ strain expressing the respective GFP–Tpk–His_6 construct after incubation for 3 h at 37 °C or 24 °C (Figure 4A), as well as the specific catalytic activity of the immunopurified GFP–Tpk–His_6 proteins (Figure 4B).

In WT cells, Tpk1 and Tpk2 interact with Bcy1 at both permissive and restrictive temperatures, as judged by the presence of co-immunoprecipitated Bcy1 protein (Figure 4A, bottom panel), as well as by the detection of cAMP-dependent kinase activity in the immunoprecipitates (Figure 4B). Compared with WT cells, *pkh1^{ts} pkh2Δ pkh3Δ* cells show reduced interaction between Tpk2 and Bcy1 even at permissive temperature. A more pronounced effect was observed at restrictive temperature, where inactivation of Pkh1 promotes a strong decrease in the Tpk2–Bcy1 interaction (Figure 4A, bottom panel). Accordingly, Tpk2 immunoprecipitated from *pkh1^{ts} pkh2Δ pkh3Δ* cells shows kinase activity that is independent of cAMP, as opposed to WT cells. As for Tpk1, we did not observe an effect on specific catalytic activity (+cAMP) of Tpk2 after Pkh1 inactivation (Figure 4B). In contrast, Tpk3 showed only very low levels of co-immunoprecipitated Bcy1, resulting in cAMP-independent kinase activity both in WT and *pkh1^{ts} pkh2Δ pkh3Δ* cells (Figure 4A and 4B).

As we have shown previously [45], measurement of PKA activity *in situ* gives a reliable indication of the *in vivo* activity of PKA. Cells expressing Tpk1 or Tpk2 show a higher dependence on cAMP than cells expressing Tpk3 (*in situ* ±cAMP activity ratio 0.02, 0.07 and 0.3 for Tpk1, Tpk2 and Tpk3 respectively; results not shown). In agreement with the results obtained by co-immunopurification, this indicates a clear difference in the degree of inhibition of Tpk1 and Tpk2 by Bcy1 compared with Tpk3. Comparison of PDK1-site phosphorylation of each Tpk compared with the amount of co-immunoprecipitated Bcy1 in WT cells (Figure 4) gives information about the requirement of a phospho-threonine residue in the activation loop to maintain the Tpk–Bcy1 interaction. The ratio of phospho-PDK1 site signal/associated Bcy1 gives the following values: 1.7 for Tpk1, 0.2 for Tpk2 and 4.0 for Tpk3. This further suggests that, in contrast with Tpk1, Pkh-mediated phosphorylation of Tpk2 is not required for association with Bcy1. On the other hand, Pkh-mediated phosphorylation of Tpk3 is not sufficient to mediate the Tpk3–Bcy1 interaction.

Taken together, the results of the present study indicate that the Pkh protein kinases are the *in vivo* upstream PDK1 site kinases for the three catalytic subunits of PKA, with the efficiency of the phosphorylation clearly differing for the isoforms. In addition, our results show that Pkh inactivation reduces the Bcy1–Tpk interaction (mainly Tpk1 and Tpk2), without affecting specific kinase activity. On the other hand, our results suggest that Pkh-mediated Tpk3 phosphorylation could not be sufficient to promote the Bcy1 interaction.

Comparative analysis of the *in vitro* interaction and phosphorylation of Tpk1, Tpk2 and Tpk3 with and by Pkh1

It has been described previously [25] that Thr^{241} in Tpk1 is the main residue targeted by Pkh1 *in vitro*. The three Tpk isoforms contain a conserved PDK1 consensus sequence in the activation loop that flanks the threonine phosphorylation site (Figure 1). In addition, the Tpk isoforms have a HM similar to that of mammalian Cα, where the phosphorylatable residue in the HM is missing. However, Tpk3 does not possess a canonical HM, since the first hydrophobic residue is replaced by a methionine residue (MKEF). To check whether Tpk2 and Tpk3 can also interact with Pkh1 through its PIF pocket, *in vitro* pull-down assays were performed by incubating Tpk1, Tpk2, Tpk3 and $Tpk3^{FXXF}$ (a mutant carrying the FKEF HM) N-terminal GST-fusion proteins purified from *E. coli*, with crude extracts obtained from yeast cells expressing either Pkh1–HA or $Pkh1^{L199E}$–HA (Figure 5).

The interaction of Tpk1 and Tpk2 with Pkh1, detected by immunoblotting with an anti-HA antibody, was reduced when the PIF pocket in Pkh1 was mutated. For Tpk3, a very weak interaction with Pkh1 was observed, that did not depend on the PIF pocket in Pkh1. The interaction of $Tpk3^{FXXF}$ with Pkh1 was slightly increased compared with Tpk3. More importantly, this canonical FXXF motif rendered Tpk3 more responsive to the presence of a functional PIF pocket in Pkh1.

An *in vitro* kinase assay was used to establish whether each Tpk could be a substrate for Pkh *in vitro*. To avoid autophosphorylation during the *in vitro* kinase reaction, an inactive version [KD (kinase dead)] of each GST–Tpk was used. GST–$Tpk1^{KD}$, GST–$Tpk2^{KD}$ or GST–$Tpk3^{KD}$, purified from *E. coli*, were individually incubated with immunopurified Pkh1–HA or $Pkh1^{KD}$–HA in the presence of [γ-^{32}P]ATP. The phosphorylation of each Tpk was detected by the incorporation of ^{32}P and expressed as the ratio ^{32}P signal/amount of protein (Figure 6). A control experiment (results not shown) showed that the amount of Pkh1–HA and $Pkh1^{KD}$–HA used was similar. The three catalytic subunits are phosphorylated by Pkh1 *in vitro*, although not to the same extent. Consistent with the Tpk–Pkh interaction results, the $Tpk3^{FXXF,KD}$ mutant, carrying a canonical HM, showed a higher phosphorylation degree compared with $Tpk3^{KD}$.

To evaluate whether the threonine residue in the activation loop is the main Pkh1 target *in vitro*, a mutant version of each Tpk, in which the corresponding threonine residue was mutated to alanine, was used (Figure 7A). The degree of phosphorylation for each Tpk was estimated by the ratio of ^{32}P incorporated for Tpk^{KD} and $Tpk^{KD,TxA}$ compared with the amount of Tpk protein (Figure 7A, right-hand panels). *In vitro* phosphorylation was drastically reduced in $Tpk1^{KD,TxA}$ confirming that Thr^{241} is the main residue targeted by Pkh1 *in vitro* [25]. Surprisingly, the $Tpk2^{KD,TxA}$ mutant still showed ^{32}P incorporation, indicating that Thr^{224} is not the only residue in Tpk2 targeted by Pkh1 *in vitro*. Hence, there appear to be additional uncharacterized Pkh1 target sites in Tpk2. Although Tpk3 is poorly phosphorylated by Pkh *in vitro*, $Tpk3^{KD,TxA}$ still shows ^{32}P incorporation by Pkh1. When the canonical HM consensus sequence is reconstituted in Tpk3, phosphorylation is increased, but on other residue(s) other than Thr^{242}. Therefore the absence of a canonical HM in Tpk3 could prevent Pkh1 to access additional sites in Tpk3.

Immunoblot analysis of GST–$Tpk2^{KD}$ and GST–$Tpk3^{KD}$ showed that Tpk2 and Tpk3 are very poorly phosphorylated

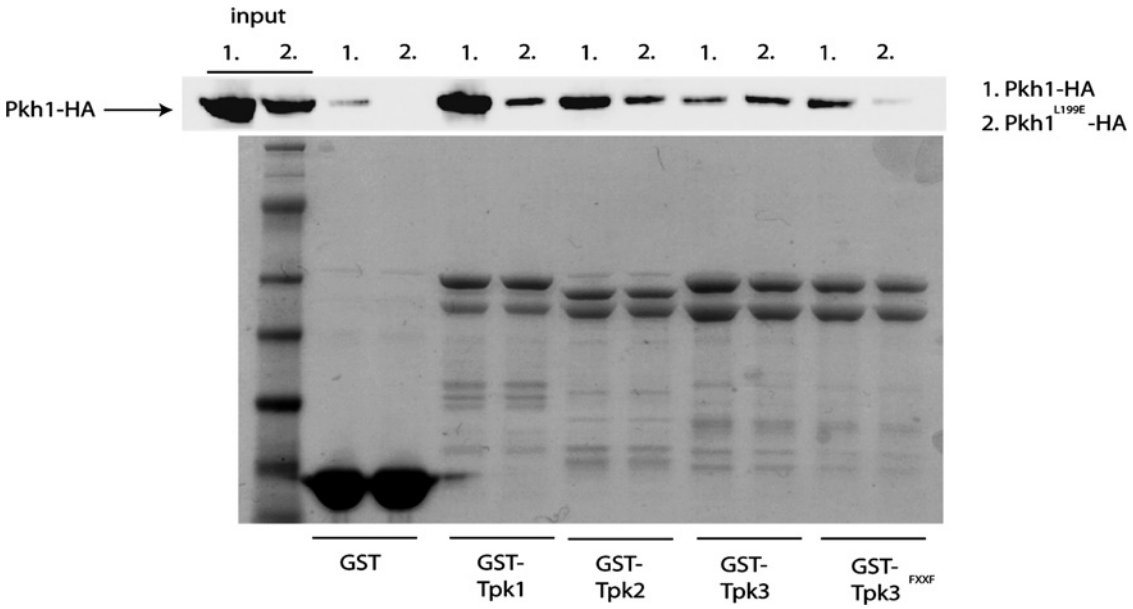

Figure 5 The hydrophobic pocket in Pkh1 is required for its interaction with the HM motif in Tpk1, Tpk2 and Tpk3 *in vitro*

Purified immobilized GST (glutathione transferase)–Tpk1, GST–Tpk2, GST–Tpk3 and GST–Tpk3^{FXXF} (FXXF corresponds to the sequence FKEF) were incubated with yeast cell extracts expressing Pkh1–HA or Pkh1^{L199E}–HA. After pull down of each Tpk, Pkh1–HA and Pkh1^{L199E}–HA were detected by immunoblotting using an anti-HA antibody. Coomassie Blue staining of a parallel gel shows similar levels of the GST–Tpks. The input fraction represents 10 % of the amount of Pkh1 added to each binding reaction.

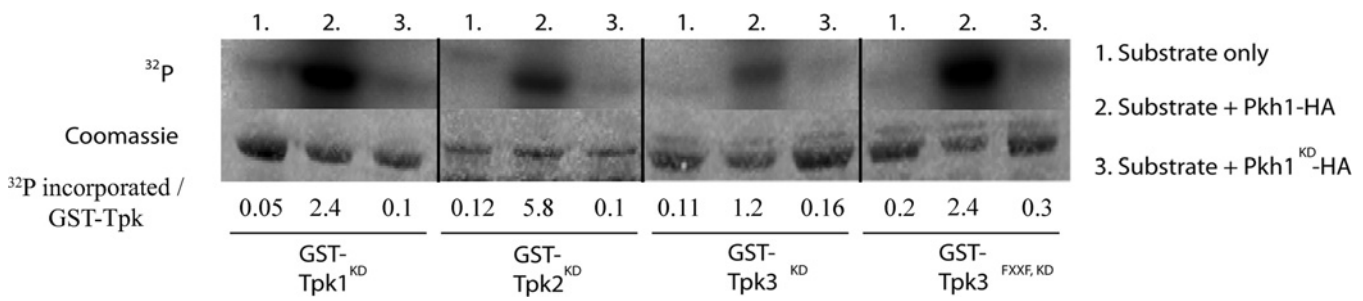

Figure 6 Different degrees of phosphorylation of Tpk1, Tpk2 and Tpk3 by Pkh1 *in vitro*

Pkh1–HA and Pkh1^{KD}–HA purified and bound to anti-HA–agarose beads resuspended in kinase buffer containing 10 μM ATP and 1 μCi of [γ-^{32}P]ATP and an aliquot of the appropriate GST–Tpk^{KD} bead-bound purified protein as a substrate. Proteins were resolved by SDS/PAGE, stained with Coomassie Blue and analysed by autoradiography. Values represent the ^{32}P incorporated/amount of GST–Tpk signal.

by active Pkh1 *in vitro* (Figure 7B). GST–Tpk1^{KD,TxA}, GST–Tpk2^{KD,TxA} and GST–Tpk3^{KD,TxA} mutant proteins were used as control. These results are in agreement with the *in vitro* ^{32}P kinase assay (Figure 7A) and the *in vivo* analysis (Figure 3).

DISCUSSION

Mechanism of phosphorylation of the activation loop residue of each Tpk by Pkh

AGC kinase activation involves phosphorylation of two highly conserved regulatory motifs: the activation loop in the catalytic domain and the HM localized in the C-terminal segment [51]. Phosphorylation of mammalian PKA on Thr^{197} is required for PKA activity [12]. Several AGC kinases in *S. cerevisiae* are activated by phosphorylation of the T-loop in their kinase domain by the Pkh protein kinases, the PDK1 homologues in budding yeast [24,25]. Sequence alignment of Tpk1, Tpk2, Tpk3 and mammalian Cα shows that the three Tpks have a conserved T-loop and truncated HM (Figure 1). Unlike Tpk1 and Tpk2, Tpk3 lacks a typical HM, since the first hydrophobic residue (phenylalanine) is replaced by methionine. The mechanism of the Pkh1–Tpk interaction as well as the Pkh1 target site in the activation loop of each Tpk has been analysed in the present study using an *in vitro* GST pull-down assay and *in vitro* kinase assay. Tpk1 and Tpk2 interact with Pkh1 principally through a mechanism that depends on an HM–PIF pocket interaction since mutagenesis of the hydrophobic pocket in Pkh1 reduces the interactions between Pkh1–Tpk1 and Pkh1–Tpk2 (Figure 8). Tpk3 shows a weak interaction with Pkh1, independent of the presence of the PIF pocket in Pkh1. This weak interaction is, in part, due to the atypical C-terminal MXXF motif in Tpk3, since

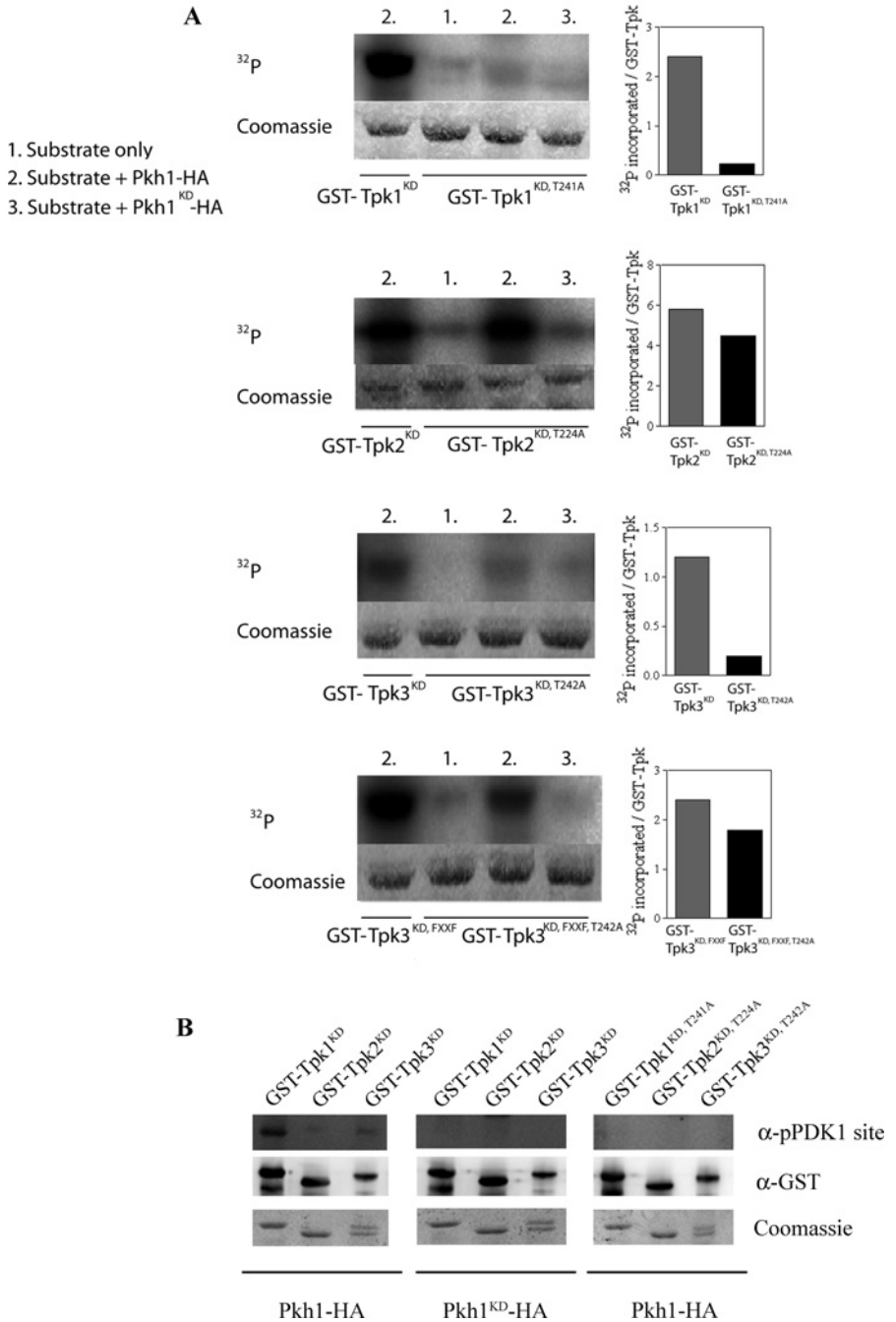

Figure 7 PDK1 site of Tpk1, but not of Tpk2 or Tpk3, is the main residue targeted by Pkh1 *in vitro*

(**A**) Bead-bound immunocomplexes from Pkh1–HA and Pkh1^{KD}–HA were resuspended in kinase buffer containing 10 μM ATP and 1 μCi of [γ-^{32}P]ATP and the appropriate bead-bound purified GST–Tpk protein as a substrate. Proteins were resolved by SDS/PAGE, stained by Coomassie Blue and analysed by autoradiography. The right-hand panel shows the ratio of ^{32}P incorporated/amount of GST–Tpk derived from densitometric analysis of the bands from reactions from incubation with Pkh1–HA (number 2). (**B**) PDK1 site phosphorylation was analysed by immunoblotting with an anti-phospho-PDK1 site antibody using equivalent samples to those shown in (**A**).

mutation of this sequence to the canonical FXXF partially restores its interaction with Pkh1, making it dependent on the HM–PIF pocket interaction.

Pkh1 phosphorylates Thr^{241} in Tpk1 [25]. Even though Tpk2 shows higher *in vitro* phosphorylation, Thr^{224} does not seem to be the major site targeted by Pkh1 *in vivo*, suggesting that Tpk2 has other, as yet uncharacterized, Pkh1 target sites. Thr^{242} in Tpk3 is poorly phosphorylated by Pkh1 due to its low interaction with Pkh1. Similar to Tpk2, Tpk3 seems to have additional Pkh1-targeted phosphorylation sites. However, sequence analysis of Tpk2 and Tpk3 does not reveal another **T**FCGT (where bold-type indicates a phosphorylatable residue) PDK1 consensus sequence. Hence Pkh1 seems to have other consensus sequences for target site phosphorylation.

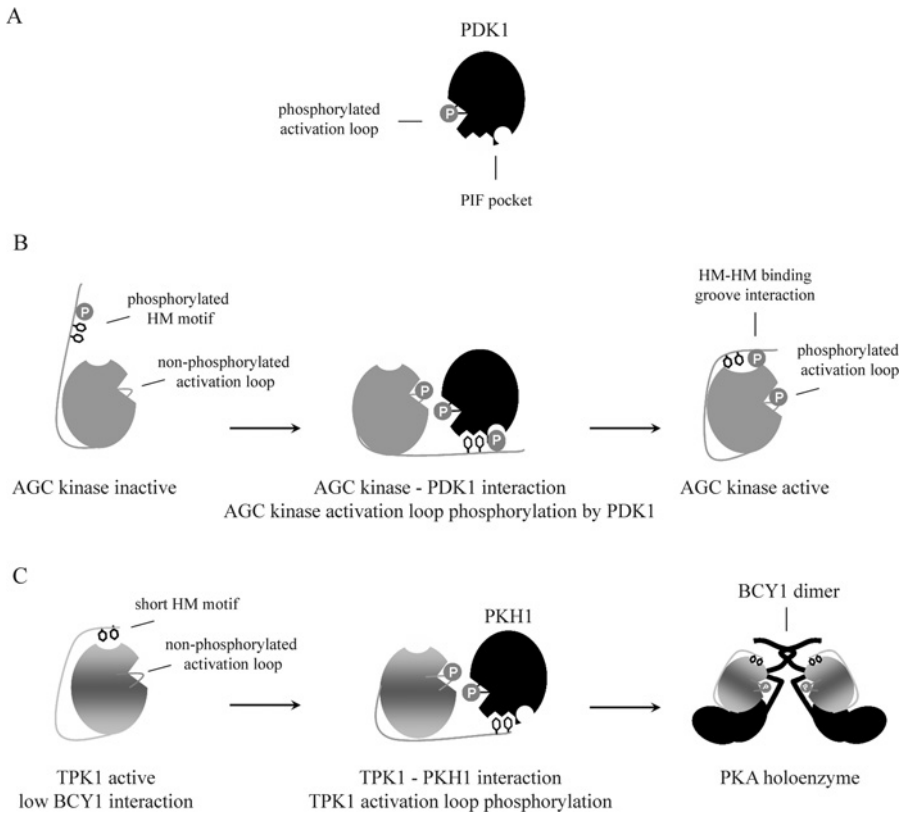

Figure 8 Mechanism of activation of AGC kinases by PDK1

(**A**) Schematic diagram of PDK1 showing the phosphorylated activation loop in the catalytic core and PIF pocket. (**B**) Once the AGC kinase C-terminal HM is phosphorylated it is recognized by PDK1 through an interaction between HM and the PIF pocket. This interaction promotes PDK1 activation resulting in phosphorylation of the AGC activation loop. AGC kinase becomes active due to the phosphorylation of its activation loop and the binding of its HM to the HM-binding groove. (**C**) The catalytic subunits of PKA possess a partial HM that ends in an FXXF motif. The non-phosphorylated activation loop conformation of TPK1 affects its association with Bcy1, rather than affecting its catalytic turnover number. The interaction of the short HM of TPK1 with the PIF pocket of PKH1 leads to phosphorylation of the activation loop of TPK1. Activation-loop-phosphorylated TPK1 is capable of interacting with the BCY1 dimer to conform the holoenzyme molecule.

The C-terminal segment of AGC kinases also contains a second phosphorylation site termed TM (turn motif) (Figure 1). While the present study was being prepared for publication, a study was published showing that *cis*-autophosphorylation of Ser^{338} occurs co-translationally, when the mammalian C-subunit is associated with ribosomes and precedes post-translational phosphorylation of the activation loop Thr^{197} [48]. Sequence alignment between the Tpks and Cα shows that the yeast catalytic subunits do not have a serine or threonine residue equivalent to Ser^{338} in the TM site of Cα (Figure 1). This observation suggests that the molecular events that regulate interaction of the Tpks with Pkh1 could be slightly different from the mechanism involved in the mammalian PKA–PDK1 interaction.

Catalytic isoforms of yeast PKA are differentially phosphorylated in a Pkh-dependent manner *in vivo* at the conserved threonine residue in the activation loop

In *S. cerevisiae*, PKA enzymatic activity is tightly regulated by the association of the catalytic subunits with the regulatory subunits, which block access to the active site. The production of cAMP, evoked by glucose addition to glucose-derepressed cells through the Gpr1/Gpa2/Ras/adenylate cyclase pathway [52], favours the dissociation of the catalytic subunits via binding to the regulatory subunits. Although the catalytic subunits are redundant for viability, they play different physiological roles. Just like mammalian cells, yeast cells can use different mechanisms to achieve specificity in PKA signalling. One conserved mechanism may involve the control of PKA activity through PDK1 site phosphorylation.

A comparative analysis of the phosphorylation state of the PDK1 site in each Tpk isoform was performed in fermenting and respiring cells. Each Tpk catalytic subunit shows a differential degree of PDK1 site phosphorylation *in vivo*, ordered as follows: Tpk1>Tpk3>Tpk2. No major differences were found in the relative phosphorylation degree of the PDK1 site in each Tpk when comparing cells grown on glucose (fermentation) or on glycerol (respiration). These observations suggest that, as is the case for Tpk1 [25], PDK1 site phosphorylation in Tpk2 and Tpk3 is not carbon-source-regulated, at least not under the conditions used in the present study.

Taking into account the stability of the different Tpk proteins (Tpk1$\approx$120 min; Tpk2 and Tpk3$\approx$80 min; results not shown) and the stable nature of PDK1 site phosphorylation, at least for Tpk1 [25,53], we had to compromise in the present study between the time of incubation at restrictive temperature of the pkh^{ts} mutant and the time required for Tpk protein synthesis. A potential concern regarding our results is that the effect of Pkh inactivation in pkh^{ts} mutant cells at restrictive temperature is not a direct effect of defective Pkh activity, but rather due to side effects on cellular functionality. There are several reasons

why this is not likely. First, upon Pkh inactivation we have not observed any protein degradation (Supplementary Figure S2, and Figures 2 and 3). Secondly, we have not observed any effect on cytoplasmic localization of Bcy1 (glycerol-growing cells; results not shown), which is dependent on Bcy1 N-terminal cluster I and II serine phosphorylation [50]. Thirdly, kinase activity measured with immunopurified Tpk (Figure 2) or measured *in situ* (Supplementary Figure S2) was similar, suggesting that cellular enzymatic activity was not affected. Finally, cell viability was not affected after incubation at the restrictive temperature of pkh^{ts} mutant cells, nor was there any indication for an apoptotic process observed (Supplementary Figure S1). These observations support the conclusion that inactivation of the Pkh protein kinases results in a direct reduction in the degree of PDK1 site phosphorylation of Tpk *in vivo*, rather than being an indirect consequence. In this regard, inactivation of the Pkh pathway after incubation at restrictive temperature also did not inhibit mRNA decay or P-body formation [54], further confirming that cellular physiological processes are not unspecifically deteriorating upon Pkh knock out.

Inactivation of the Pkh protein kinases decreases phosphorylation of the PDK1 site in all three Tpk isoforms, indicating that Pkh kinase activity is required for PDK1 site phosphorylation of the three isoforms *in vivo*. Since Pkh-mediated phosphorylation of Tpk1 occurs during the synthesis of new Tpk1, and since the phosphate group introduced seems to be phosphatase-resistant, we believe that the temperature shift in the pkh^{ts} strain triggers reduction of PDK1 site *de novo* phosphorylation rather than stimulating its dephosphorylation. The possibility of other kinases phosphorylating Thr^{241} or of Tpk1 autophosphorylating this site is minimized if we take into account that several kinase mutants did not affect PDK1 site phosphorylation [25] and GST–Tpk1 did not autophosphorylate in bacteria (results not shown). The stability of Tpk1 in combination with the stable nature of Thr^{241} phosphorylation are reasonable explanations for the residual phosphorylation of Thr^{241} observed after Pkh inactivation.

In yeast and mammalian cells, the residues that are required for the interaction between catalytic and regulatory subunits of PKA are conserved (results not shown). Specifically, threonine at position 241 in the activation loop is important for the tight interaction between the catalytic and regulatory subunit in the absence of cAMP [37]. Although the best-established mechanism for PKA regulation is its activation through binding of cAMP to the regulatory subunits, previous studies have suggested that PKA could be regulated by other mechanisms [21–23]. In the present study, a universal correlation between Pkh-mediated PDK1 site phosphorylation of the Tpks and their interaction with Bcy1 is not observed, suggesting that not all three Tpk isoforms require PDK1 site phosphorylation to maintain the Tpk–Bcy1 interaction. In contrast with Tpk1 (Figure 8), PDK1 site phosphorylation in Tpk2 is not required for its association with Bcy1. In addition, *in vitro* results indicate that Tpk2 can be phosphorylated by Pkh1 on other target site(s). We speculate that phosphorylation by the Pkh protein kinases of these uncharacterized residue(s) could be responsible for supporting association of Tpk2 with Bcy1. On the other hand, phosphorylation of the PDK1 site in Tpk3 is not sufficient to mediate the Tpk3–Bcy1 interaction. On the basis of our *in vitro* and *in vivo* results, we speculate that Tpk3 could be the isoform with the lowest affinity for Bcy1. The *in vitro* results suggest that the atypical HM at the C-terminus of Tpk3 is most likely to be the reason for the reduced phosphorylation of the threonine residue in its activation loop *in vivo*, and is a consequence of a reduced Tpk3–Pkh interaction. These findings indicate that Tpk3 is poorly regulated by the Pkh protein kinases and by Bcy1.

It has been shown previously that all three catalytic subunits have a similar specific activity towards kemptide and protein substrates *in vitro* [55], indicating that low *in vivo* Tpk3 activity is not due to low catalytic activity of the protein. Low expression [56] and/or sequestration in ribonucleoprotein granules [47] could be regulatory mechanisms lowering Tpk3 catalytic activity.

The precise role of the Pkh protein kinases in controlling *in vivo* PKA activity has been very difficult to address experimentally, mainly for two reasons. First, since the Pkh protein kinases are master kinases that control several downstream AGC kinase activities, the evaluation of phenotypic readouts controlled by PKA after Pkh inactivation, using the pkh^{ts} allele or inhibitors [57], can be compromised by indirect effects. Secondly, as we have demonstrated, mutation of Tpk1 Thr^{241} to an unphosphorylatable residue has other consequences on the functionality of the protein than those caused by the absence of the phosphate group. In spite of this, we have been able to demonstrate that the Pkh protein kinases are the PDK1 site kinases for all three catalytic subunits of PKA in budding yeast. The phosphorylation occurs with different efficiency for each catalytic subunit, which may be relevant for establishing several Tpk-specific properties, dependent or not on Bcy1. Hence, the findings of the present study suggest for the first time that a common upstream kinase may contribute to divergence in cAMP-dependent regulation of PKA isoforms.

AUTHOR CONTRIBUTION

Steven Haesendonckx and Vanesa Tudisca designed and performed experiments. Karin Voordeckers, Silvia Moreno and Johan M. Thevelein provided critical insight into data interpretation and contributed to the writing of the paper. Paula Portela designed and performed experiments, analysed data and wrote the paper.

ACKNOWLEDGMENTS

We thank K. Irie and J. Thorner for the gift of strains and plasmids.

FUNDING

This work was supported by a Ph.D. fellowship from the Fund for Scientific Research-Flanders (FWO) (to K.V.), a fellowship from the Agency for Innovation by Science and Technology (IWT-Flanders) (to S.H.), by a Ph.D. fellowship from the University of Buenos Aires (UBA) (to V.T.), and by grants from the Fund for Scientific Research-Flanders, the Interuniversity Attraction Poles Network P6/14 and the Research-Fund of the KULeuven (Concerted Research Actions) (to J.M.T.), the Agencia Nacional de Promoción Científica y Tecnológica [grant number PICT 2195], the University of Buenos Aires [grant number UBA X-528] and from Consejo Nacional de Investigaciones Científicas y Técnicas (CONICET) [grant number PIP 0519].

REFERENCES

1 Manning, G., Whyte, D. B., Martinez, R., Hunter, T. and Sudarsanam, S. (2002) The protein kinase complement of the human genome. Science **298**, 1912–1934
2 Hanks, S. K. and Hunter, T. (1995) Protein kinases 6. The eukaryotic protein kinase superfamily: kinase (catalytic) domain structure and classification. FASEB J. **9**, 576–596
3 Johnson, L. N., Noble, M. E. and Owen, D. J. (1996) Active and inactive protein kinases: structural basis for regulation. Cell **85**, 149–158
4 Casamayor, A., Torrance, P. D., Kobayashi, T., Thorner, J. and Alessi, D. R. (1999) Functional counterparts of mammalian protein kinases PDK1 and SGK in budding yeast. Curr. Biol. **9**, 186–197
5 Vanhaesebroeck, B. and Alessi, D. R. (2000) The PI3K-PDK1 connection: more than just a road to PKB. Biochem. J. **346**, 561–576
6 Biondi, R. M., Cheung, P. C., Casamayor, A., Deak, M., Currie, R. A. and Alessi, D. R. (2000) Identification of a pocket in the PDK1 kinase domain that interacts with PIF and the C-terminal residues of PKA. EMBO J. **19**, 979–988

7 Biondi, R. M., Komander, D., Thomas, C. C., Lizcano, J. M., Deak, M., Alessi, D. R. and van Aalten, D. M. (2002) High resolution crystal structure of the human PDK1 catalytic domain defines the regulatory phosphopeptide docking site. EMBO J. **21**, 4219–4228

8 Frodin, M., Antal, T. L., Dummler, B. A., Jensen, C. J., Deak, M., Gammeltoft, S. and Biondi, R. M. (2002) A phosphoserine/threonine-binding pocket in AGC kinases and PDK1 mediates activation by hydrophobic motif phosphorylation. EMBO J. **21**, 5396–5407

9 Collins, B. J., Deak, M., Arthur, J. S., Armit, L. J. and Alessi, D. R. (2003) *In vivo* role of the PIF-binding docking site of PDK1 defined by knock-in mutation. EMBO J. **22**, 4202–4211

10 Frodin, M., Jensen, C. J., Merienne, K. and Gammeltoft, S. (2000) A phosphoserine-regulated docking site in the protein kinase RSK2 that recruits and activates PDK1. EMBO J. **19**, 2924–2934

11 Keshwani, M. M., von Daake, S., Newton, A. C., Harris, T. K. and Taylor, S. S. (2011) Hydrophobic motif phosphorylation is not required for activation loop phosphorylation of p70 ribosomal protein S6 kinase 1 (S6K1). J. Biol. Chem. **286**, 23552–23558

12 Cheng, X., Ma, Y., Moore, M., Hemmings, B. A. and Taylor, S. S. (1998) Phosphorylation and activation of cAMP-dependent protein kinase by phosphoinositide-dependent protein kinase. Proc. Natl. Acad. Sci. U.S.A. **95**, 9849–9854

13 Iyer, G. H., Garrod, S., Woods, Jr, V. L. and Taylor, S. S. (2005) Catalytic independent functions of a protein kinase as revealed by a kinase-dead mutant: study of the Lys72His mutant of cAMP-dependent kinase. J. Mol. Biol. **351**, 1110–1122

14 Moore, M. J., Kanter, J. R., Jones, K. C. and Taylor, S. S. (2002) Phosphorylation of the catalytic subunit of protein kinase A. Autophosphorylation versus phosphorylation by phosphoinositide-dependent kinase-1. J. Biol. Chem. **277**, 47878–47884

15 Williams, M. R., Arthur, J. S., Balendran, A., van der Kaay, J., Poli, V., Cohen, P. and Alessi, D. R. (2000) The role of 3-phosphoinositide-dependent protein kinase 1 in activating AGC kinases defined in embryonic stem cells. Curr. Biol. **10**, 439–448

16 Batkin, M., Schvartz, I. and Shaltiel, S. (2000) Snapping of the carboxyl terminal tail of the catalytic subunit of PKA onto its core: characterization of the sites by mutagenesis. Biochemistry **39**, 5366–5373

17 Steichen, J. M., Iyer, G. H., Li, S., Saldanha, S. A., Deal, M. S., Woods, Jr, V. L. and Taylor, S. S. (2010) Global consequences of activation loop phosphorylation on protein kinase A. J. Biol. Chem. **285**, 3825–3832

18 Nirula, A., Ho, M., Phee, H., Roose, J. and Weiss, A. (2006) Phosphoinositide-dependent kinase 1 targets protein kinase A in a pathway that regulates interleukin 4. J. Exp. Med. **203**, 1733–1744

19 Hirimburegama, K., Durnez, P., Keleman, J., Oris, E., Vergauwen, R., Mergelsberg, H. and Thevelein, J. M. (1992) Nutrient-induced activation of trehalase in nutrient-starved cells of the yeast *Saccharomyces cerevisiae*: cAMP is not involved as second messenger. J. Gen. Microbiol. **138**, 2035–2043

20 Durnez, P., Pernambuco, M. B., Oris, E., Arguelles, J. C., Mergelsberg, H. and Thevelein, J. M. (1994) Activation of trehalase during growth induction by nitrogen sources in the yeast *Saccharomyces cerevisiae* depends on the free catalytic subunits of cAMP-dependent protein kinase, but not on functional Ras proteins. Yeast **10**, 1049–1064

21 Lu, A. and Hirsch, J. P. (2005) Cyclic AMP-independent regulation of protein kinase A substrate phosphorylation by Kelch repeat proteins. Eukaryotic Cell **4**, 1794–1800

22 Peeters, T., Louwet, W., Gelade, R., Nauwelaers, D., Thevelein, J. M. and Versele, M. (2006) Kelch-repeat proteins interacting with the Gα protein Gpa2 bypass adenylate cyclase for direct regulation of protein kinase A in yeast. Proc. Natl. Acad. Sci. U.S.A. **103**, 13034–13039

23 Budhwar, R., Lu, A. and Hirsch, J. P. (2010) Nutrient control of yeast PKA activity involves opposing effects on phosphorylation of the Bcy1 regulatory subunit. Mol. Biol. Cell **21**, 3749–3758

24 Inagaki, M., Schmelzle, T., Yamaguchi, K., Irie, K., Hall, M. N. and Matsumoto, K. (1999) PDK1 homologs activate the Pkc1-mitogen-activated protein kinase pathway in yeast. Mol. Cell. Biol. **19**, 8344–8352

25 Voordeckers, K., Kimpe, M., Haesendonckx, S., Louwet, W., Versele, M. and Thevelein, J. M. (2011) Yeast 3-phosphoinositide-dependent protein kinase-1 (PDK1) orthologs, Pkh1–3, differentially regulate phosphorylation of PKA and the PKB/S6K ortholog, Sch9. J. Biol. Chem. **286**, 22017–22027

26 De Camilli, P., Emr, S. D., McPherson, P. S. and Novick, P. (1996) Phosphoinositides as regulators in membrane traffic. Science **271**, 1533–1539

27 Gallego, O., Betts, M. J., Gvozdenovic-Jeremic, J., Maeda, K., Matetzki, C., Aguilar-Gurrieri, C., Beltran-Alvarez, P., Bonn, S., Fernandez-Tornero, C., Jensen, L. J. et al. (2010) A systematic screen for protein-lipid interactions in *Saccharomyces cerevisiae*. Mol. Syst. Biol. **6**, 430

28 Dickson, R. C. (2010) Roles for sphingolipids in *Saccharomyces cerevisiae*. Adv. Exp. Med. Biol. **688**, 217–231

29 Friant, S., Lombardi, R., Schmelzle, T., Hall, M. N. and Riezman, H. (2001) Sphingoid base signaling via Pkh kinases is required for endocytosis in yeast. EMBO J. **20**, 6783–6792

30 deHart, A. K., Schnell, J. D., Allen, D. A. and Hicke, L. (2002) The conserved Pkh-Ypk kinase cascade is required for endocytosis in yeast. J. Cell Biol. **156**, 241–248

31 Grosshans, B. L., Grotsch, H., Mukhopadhyay, D., Fernandez, I. M., Pfannstiel, J., Idrissi, F. Z., Lechner, J., Riezman, H. and Geli, M. I. (2006) TEDS site phosphorylation of the yeast myosins I is required for ligand-induced but not for constitutive endocytosis of the G protein-coupled receptor Ste2p. J. Biol. Chem. **281**, 11104–11114

32 Zhang, X., Lester, R. L. and Dickson, R. C. (2004) Pil1p and Lsp1p negatively regulate the 3-phosphoinositide-dependent protein kinase-like kinase Pkh1p and downstream signaling pathways Pkc1p and Ypk1p. J. Biol. Chem. **279**, 22030–22038

33 Dickson, R. C., Sumanasekera, C. and Lester, R. L. (2006) Functions and metabolism of sphingolipids in *Saccharomyces cerevisiae*. Prog. Lipid Res. **45**, 447–465

34 Daquinag, A., Fadri, M., Jung, S. Y., Qin, J. and Kunz, J. (2007) The yeast PH domain proteins Slm1 and Slm2 are targets of sphingolipid signaling during the response to heat stress. Mol. Cell. Biol. **27**, 633–650

35 Walther, T. C., Aguilar, P. S., Frohlich, F., Chu, F., Moreira, K., Burlingame, A. L. and Walter, P. (2007) Pkh-kinases control eisosome assembly and organization. EMBO J. **26**, 4946–4955

36 Luo, G., Gruhler, A., Liu, Y., Jensen, O. N. and Dickson, R. C. (2008) The sphingolipid long-chain base-Pkh1/2-Ypk1/2 signaling pathway regulates eisosome assembly and turnover. J. Biol. Chem. **283**, 10433–10444

37 Levin, L. R. and Zoller, M. J. (1990) Association of catalytic and regulatory subunits of cyclic AMP-dependent protein kinase requires a negatively charged side group at a conserved threonine. Mol. Cell. Biol. **10**, 1066–1075

38 Gruhler, A., Olsen, J. V., Mohammed, S., Mortensen, P., Faergeman, N. J., Mann, M. and Jensen, O. N. (2005) Quantitative phosphoproteomics applied to the yeast pheromone signaling pathway. Mol. Cell. Proteomics **4**, 310–327

39 Bodenmiller, B. and Aebersold, R. (2010) Quantitative analysis of protein phosphorylation on a system-wide scale by mass spectrometry-based proteomics. Methods Enzymol. **470**, 317–334

40 Gietz, R. D., Schiestl, R. H., Willems, A. R. and Woods, R. A. (1995) Studies on the transformation of intact yeast cells by the LiAc/SS-DNA/PEG procedure. Yeast **11**, 355–360

41 Kucsera, J., Yarita, K. and Takeo, K. (2000) Simple detection method for distinguishing dead and living yeast colonies. J. Microbiol. Methods **41**, 19–21

42 Madeo, F., Frohlich, E. and Frohlich, K. U. (1997) A yeast mutant showing diagnostic markers of early and late apoptosis. J. Cell Biol. **139**, 729–734

43 Portela, P., Howell, S., Moreno, S. and Rossi, S. (2002) *In vivo* and *in vitro* phosphorylation of two isoforms of yeast pyruvate kinase by protein kinase A. J. Biol. Chem. **277**, 30477–30487

44 Roskoski, Jr, R. (1983) Assays of protein kinase. Methods Enzymol. **99**, 3–6

45 Portela, P., Van Dijck, P., Thevelein, J. M. and Moreno, S. (2003) Activation state of protein kinase A as measured in permeabilised *Saccharomyces cerevisiae* cells correlates with PKA-controlled phenotypes *in vivo*. FEMS Yeast Res. **3**, 119–126

46 Portela, P. and Moreno, S. (2006) Glucose-dependent activation of protein kinase A activity in *Saccharomyces cerevisiae* and phosphorylation of its TPK1 catalytic subunit. Cell. Signaling **18**, 1072–1086

47 Tudisca, V., Recouvreux, V., Moreno, S., Boy-Marcotte, E., Jacquet, M. and Portela, P. (2010) Differential localization to cytoplasm, nucleus or P-bodies of yeast PKA subunits under different growth conditions. Eur. J. Cell Biol. **89**, 339–348

48 Keshwani, M. M., Klammt, C., von Daake, S., Ma, Y., Kornev, A. P., Choe, S., Insel, P. A. and Taylor, S. S. (2012) Cotranslational cis-phosphorylation of the COOH-terminal tail is a key priming step in the maturation of cAMP-dependent protein kinase. Proc. Natl. Acad. Sci. U.S.A. **109**, E1221–E1229

49 Griffioen, G., Anghileri, P., Imre, E., Baroni, M. D. and Ruis, H. (2000) Nutritional control of nucleocytoplasmic localization of cAMP-dependent protein kinase catalytic and regulatory subunits in *Saccharomyces cerevisiae*. J. Biol. Chem. **275**, 1449–1456

50 Griffioen, G., Branduardi, P., Ballarini, A., Anghileri, P., Norbeck, J., Baroni, M. D. and Ruis, H. (2001) Nucleocytoplasmic distribution of budding yeast protein kinase A regulatory subunit Bcy1 requires Zds1 and is regulated by Yak1-dependent phosphorylation of its targeting domain. Mol. Cell. Biol. **21**, 511–523

51 Dettori, R., Sonzogni, S., Meyer, L., Lopez-Garcia, L. A., Morrice, N. A., Zeuzem, S., Engel, M., Piiper, A., Neimanis, S., Frodin, M. and Biondi, R. M. (2009) Regulation of the interaction between protein kinase C-related protein kinase 2 (PRK2) and its upstream kinase, 3-phosphoinositide-dependent protein kinase 1 (PDK1). J. Biol. Chem. **284**, 30318–30327

52 Thevelein, J. M. and de Winde, J. H. (1999) Novel sensing mechanisms and targets for the cAMP-protein kinase A pathway in the yeast *Saccharomyces cerevisiae*. Mol. Microbiol. **33**, 904–918

53 Jurica, M. S., Mesecar, A., Heath, P. J., Shi, W., Nowak, T. and Stoddard, B. L. (1998) The allosteric regulation of pyruvate kinase by fructose-1,6-bisphosphate. Structure **6**, 195–210

54 Guang, S., Bochner, A. F., Burkhart, K. B., Burton, N., Pavelec, D. M. and Kennedy, S. (2010) Small regulatory RNAs inhibit RNA polymerase II during the elongation phase of transcription. Nature **465**, 1097–1101

55 Galello, F., Portela, P., Moreno, S. and Rossi, S. (2010) Characterization of substrates that have a differential effect on *Saccharomyces cerevisiae* protein kinase A holoenzyme activation. J. Biol. Chem. **285**, 29770–29779

56 Mazon, M. J., Behrens, M. M., Morgado, E. and Portillo, F. (1993) Low activity of the yeast cAMP-dependent protein kinase catalytic subunit Tpk3 is due to the poor expression of the TPK3 gene. Eur. J. Biochem. **213**, 501–506

57 Baxter, B. K., DiDone, L., Ogu, D., Schor, S. and Krysan, D. J. (2011) Identification, *in vitro* activity and mode of action of phosphoinositide-dependent-1 kinase inhibitors as antifungal molecules. ACS Chem. Biol. **6**, 502–510

Received 2 July 2012/6 September 2012; accepted 7 September 2012
Published as BJ Immediate Publication 7 September 2012, doi:10.1042/BJ20121061

Biochem. J. (2012) **448**, 307–320 (Printed in Great Britain) doi:10.1042/BJ20121061

online data

SUPPLEMENTARY ONLINE DATA

The activation loop of PKA catalytic isoforms is differentially phosphorylated by Pkh protein kinases in *Saccharomyces cerevisiae*

Steven HAESENDONCKX*†‡[1], Vanesa TUDISCA§[1], Karin VOORDECKERS†‡‖, Silvia MORENO§, Johan M. THEVELEIN†‡ and Paula PORTELA§[2]

*Department of Molecular Biology, University of Geneva CH-1211, Switzerland, †Laboratory of Molecular Cell Biology, Institute of Botany and Microbiology, KU Leuven, Kasteelpark Arenberg 31. B-3001 Leuven-Heverlee, Flanders, Belgium, ‡Department of Molecular Microbiology, VIB, Leuven-Heverlee, Flanders, Belgium, §Departamento de Química Biológica, Facultad de Ciencias Exactas y Naturales, Universidad de Buenos Aires, Ciudad Universitaria, Pabellón 2, Buenos Aires 1428, Argentina, and ‖VIB Laboratory for Systems Biology, Gaston Geenslaan 1, B-3001 Leuven, Belgium

Table S1 Yeast strains used in the present study

Strain name	Genotype	Source
15 Dau (WT)	*MATa leu2 ura3 trp1 his2 ade1*	[1]
BY4742	*MATα his3 leu2 lys2 ura3*	[2]
BJ2168	*MATα prc1-407 prb1-1122 pep4-3 leu2 trp1 ura3-52*	J. Thorner
pkh1^{ts}pkh2Δpkh3Δ	15 Dau *pkh1::PKH1D398G pkh2::LEU2 pkh3::KanMX*	K. Voordeckers
JT20570	BY4742 *Mata ade2 trp1 leu2 his3 bcy1::URA3*	J. Thevelein
KV28	BY4742 *tpk1::KanMX tpk2::KanMX tpk3::LEU2* pRS313-*TPK1*	K. Voordeckers
KV29	BY4742 *tpk1::KanMX tpk2::KanMX tpk3::LEU2* pRS313-*TPK1^{T241A}*	K. Voordeckers

Table S2 Plasmids used in the present study

Plasmid	Protein	Source
pGEX-4X-1	GST	GE Healthcare
pGEX-3X-Tpk1	GST–Tpk1	K. Voordeckers
pGEX-4X-Tpk2	GST–Tpk2	The present study
pGEX-4X-Tpk3	GST–Tpk3	The present study
pGEX-3X-Tpk1^{K116M}	GST–Tpk1^{KD}	K. Voordeckers
pGEX-3X-Tpk1$^{K116M, T241A}$	GST–Tpk1$^{KD, T241A}$	K. Voordeckers
pGEX-4X-Tpk2^{K99M}	GST–Tpk2^{KD}	The present study
pGEX-4X-Tpk2$^{K99M, T224A}$	GST–Tpk2$^{KD, T224A}$	The present study
pGEX-4X-Tpk3^{K117M}	GST–Tpk3^{KD}	The present study
pGEX-4X-Tpk3^{K117M,T242A}	GST–Tpk3^{KD,T242A}	The present study
pGEX-4X-Tpk3 ^{M395F}	GST–Tpk3 ^{FXXF}†	The present study
pGEX-4X-Tpk3$^{K117M, M395F}$	GST–Tpk3$^{KD, FXXF}$	The present study
pGEX-4X-Tpk3$^{K117M, M395F, T242A}$	GST–Tpk3$^{KD, FXXF, T242A}$	The present study
Yep351pGAL-Pkh1-HA	2μ, *LEU2*, *GAL*-Pkh1–HA	J. Thorner
Yep351pGAL- Pkh1^{K154R} -HA*	2μ, *LEU2*, *GAL*-Pkh1 ^{KD}–HA	J. Thorner
Yep351pGAL- Pkh1^{L199E} -HA*	2μ, *LEU2*, *GAL*-Pkh1 ^{L199E}–HA	K. Voordeckers
Ycplac33-pAGHTpk1	*URA3*, *ADH1-GFP-HA$_3$*-Tpk1	K. Voordeckers
Ycplac33-pAGHTpk1^{T241A}	*URA3*, *ADH1-GFP-HA$_3$*-Tpk1^{T241A}	K. Voordeckers
pBEVYU-GFP-Tpk1-His$_6$	*URA3*, *ADH1-GFP-TPK1-His$_6$*	The present study
pBEVYU-GFP-Tpk2 His$_6$	*URA3*, *ADH1-GFP-TPK2-His$_6$*	The present study
pBEVYU-GFP-Tpk3 His$_6$	*URA3*, *ADH1-GFP-TPK3-His$_6$*	The present study
YCplac33-Bcy1-GFP	*URA3, pBCY1-BCY1-GFP*	P. Portela

*Derived from YEp351GAL
†FXXF corresponds to the sequence FKEF

[1] These authors contributed equally to this work.
[2] To whom correspondence should be addressed (email pportela@qb.fcen.uba.ar).

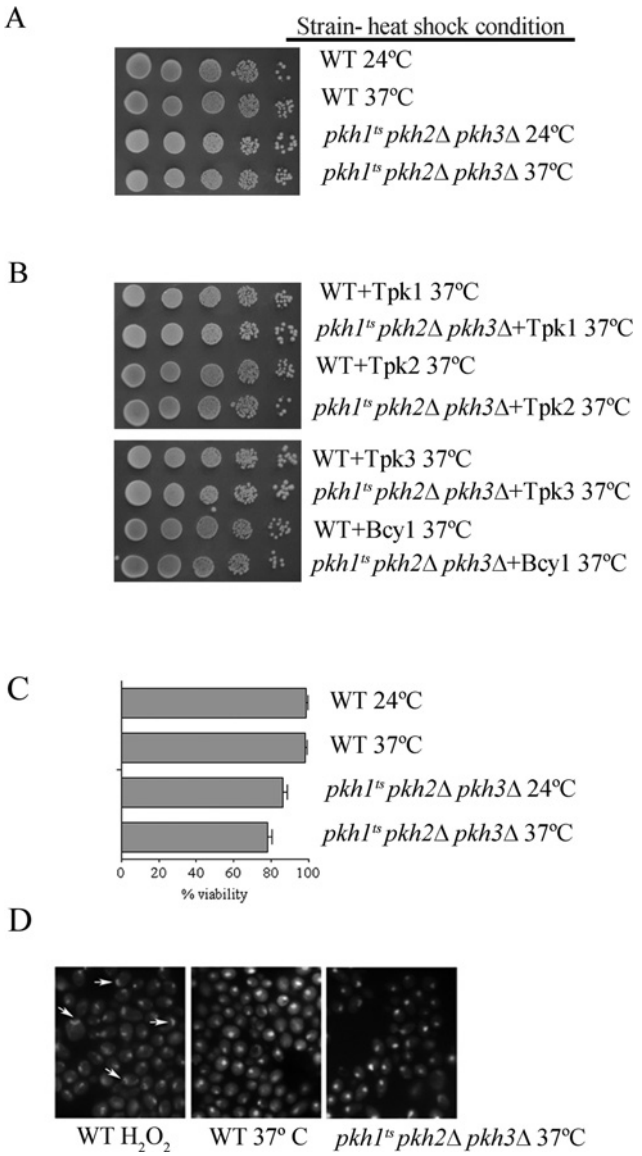

Figure S1 *pkh1^{ts}pkh2Δpkh3Δ* viability is not affected after heat shock for 3 h at 37°C

(**A**) Cells from the WT and *pkh1^{ts}pkh2Δpkh3Δ* strains and (**B**) cells from the WT and *pkh1^{ts}pkh2Δpkh3Δ* strains expressing GFP–Tpk1–His_6, GFP–Tpk2–His_6, GFP–Tpk3–His_6 or Bcy1–GFP were grown in SD-Glu for 16 h at 24°C and then shifted to 37°C for 3 h. Aliquots of the same culture were maintained at 24°C as a control. After heat-shock treatment, cell viability was verified by a spot assay of serial dilutions on agar plates. (**C**) Viability of WT or *pkh1^{ts}pkh2Δpkh3Δ* cells after incubation at restrictive temperature. Dead cells stained by Trypan Blue were visualized and counted by microscopy. The percentage viability represents the proportion of viable cells. (**D**) DAPI-stained WT yeast cells after incubation for 3 h with 3 mM H_2O_2, and WT and *pkh1^{ts}pkh2Δpkh3Δ* cells after incubation for 3 h at 37°C. The arrows show apoptotic cells induced by H_2O_2.

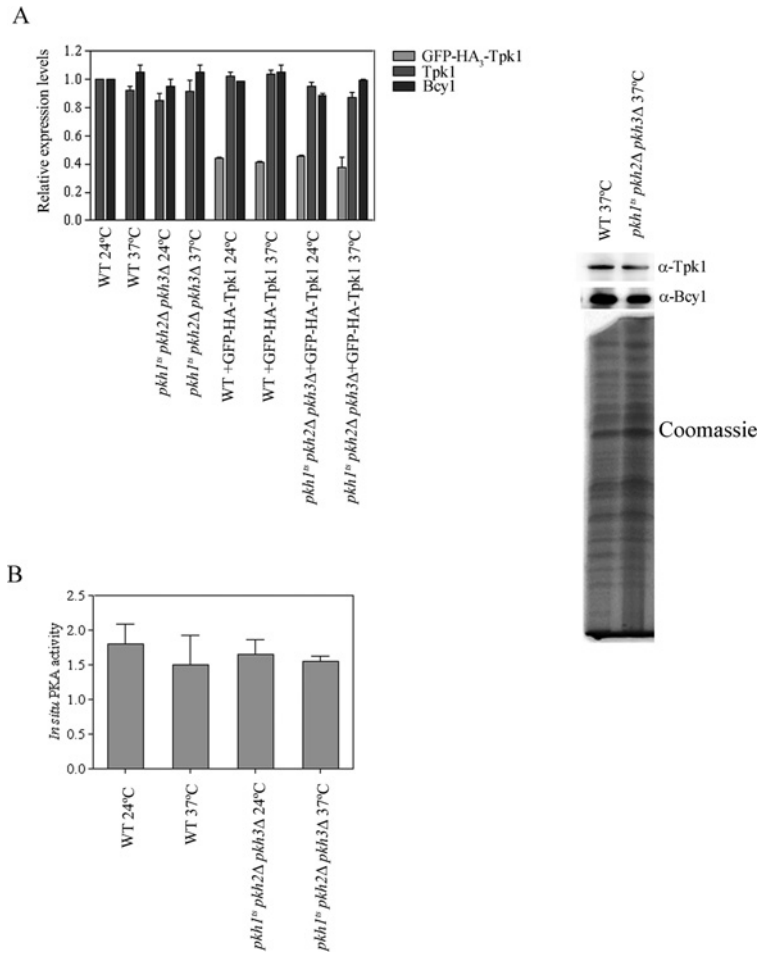

Figure 2 PKA catalytic subunit levels expression and *in situ* kinase activity

(**A**) Crude extracts from the indicated strains were prepared under the conditions detailed in the Figure and subjected to SDS/PAGE. The protein level of the Tpk1 subunit (expressed from its chromosomal location) and GST–HA–Tpk1 subunit (expressed from Ycplac50-pAGH-*GFP-HA*$_3$*-Tpk1*) was determined using an anti-Tpk1 antibody. The histogram shows the densitometric quantification of Tpk1 signal relative to the total amount of protein loaded. Expression levels of the Bcy1 subunit was determined using an anti-Bcy1 antibody. Tpk1 and Bcy1 protein levels detected in different strains/conditions were normalized to Tpk1 and Bcy1 detected in the WT strain grown at 24°C respectively taken as 1. A representative Western blot and protein pattern observed after SDS/PAGE Coomassie Blue staining is shown in the right-hand panel. (**B**) *In situ* PKA activity (+cAMP) was measured in WT and *pkh1*^{ts}*pkh2Δpkh3Δ* cells after incubation for 3 h at 37°C or maintained at 24°C and was determined as described in Experimental section of the main text.

REFERENCES

1 Inagaki, M., Schmelzle, T., Yamaguchi, K., Irie, K., Hall, M. N. and Matsumoto, K. (1999) PDK1 homologs activate the Pkc1-mitogen-activated protein kinase pathway in yeast. Mol. Cell. Biol. **19**, 8344–8352

2 Brachmann, C. B., Davies, A., Cost, G. J., Caputo, E., Li, J., Hieter, P. and Boeke, J. D. (1998) Designer deletion strains derived from *Saccharomyces cerevisiae* S288C: a useful set of strains and plasmids for PCR-mediated gene disruption and other applications. Yeast **14**, 115–132

Received 2 July 2012/6 September 2012; accepted 7 September 2012
Published as BJ Immediate Publication 7 September 2012, doi:10.1042/BJ20121061